1

1

The role of light as vital effect on coral skeleton oxygen

isotopic ratio

4

Anne Juillet-Leclerc

LSCE Domaine du CNRS, 91198 Gif-sur-Yvette, France

Correspondence to: Anne.Juillet-Leclerc@lsce.ipsl.fr
8
9

Abstract

Light, an environmental parameter playing a crucial role in coral aragonite growth and $\delta^{18}O$

formulation, is always neglected in the geochemical literature. However, by revisiting already

published studies, we demonstrated that light might be considered as a vital effect affecting coral

aragonite oxygen isotopic ratios.

Re-examining data series included in a publication by Weber and Woodhead (1972), we stressed that

annual $\delta^{18}O$–annual temperature calibrations of all considered coral genera may be compared because

their assessment assumes homogenous light levels. Temperature prevails on $\delta^{18}O$ because it influences

$\delta^{18}O$ in two ways: firstly it acts as is thermodynamically predicted implying a $\delta^{18}O$ decrease; and

secondly it induces an enhancement of photosynthesis causing $\delta^{18}O$ increase. When the highest annual

temperature occurs simultaneously with the highest annual irradiation, the annual $\delta^{18}O$ amplitude is

shortened. The annual $\delta^{18}O$–annual temperature calibration is also explained by the relative

distribution of microstructures, centres of calcification or COC and fibers, according to morphology,

and in turn taxonomy. We also investigated monthly $\delta^{18}O$–monthly temperature calibrations of *Porites*

grown at the same sites as by Stephans and Quinn (2002), Linsley et al. (1999, 2000) and Maier et al.

(2004). Multiple evidence showed that temperature is the prevailing environment forcing on $\delta^{18}O$ and

that the mixture of temperature and light also determines the relative distribution of microstructures,

27 explaining the relationships between *Porites* calibration constants. By examining monthly and annual

28 $\delta^{18}O$–monthly and annual temperature calibrations, we revealed that monthly calibration results from

29 the superimposition of seasonal and annual variability over time. Seasonal $\delta^{18}O$ strongly impacted by

30 seasonal light fluctuations, may be obtained by removing interannual $\delta^{18}O$ only weakly affected by

31 light. Such features necessitate the reconstitution of tools frequently utilised, such as the coupled

32 $\delta^{18}O$–Sr/Ca or pseudo-coral concepts.

33
34 **1 Introduction**

35 The oxygen isotope data preserved in the scleractinian coral skeleton is an excellent proxy for

36 temperature and/or $\delta^{18}O_{seawater}$ variability (McConnaughey, 1989), following the concept of isotopic

37 thermometer (Urey, 1947). However, coral aragonite $\delta^{18}O$ is depleted relative to the isotopic values of

38 the ambient seawater (Weber and Woodhead, 1972), inducing anomalies commonly termed as vital

39 effects. Therefore, we need to identify environmental parameters really included in the $\delta^{18}O$ time-

40 series, the most-used coral skeleton proxy so far.

41 Because temperature and light intensities are always strongly related in the field, the real impact of

42 light on $\delta^{18}O$ cannot be decoupled from the temperature effect. Although the relationship between

43 light and calcification has long been recognised (Goreau, 1959; Gattuso et al., 1999), the control of

44 ambient light level on the isotopic disequilibrium offset of coral aragonite from seawater could only be

45 speculated upon (Land et al., 1975; McConnaughey, 1989; Felis, 2003). The role of light on coral $\delta^{18}O$

46 can only be proved from evidence provided by cultured corals in controlled light conditions, all the

47 other parameters remaining constant (Reynaud-Vaganay et al., 2001; Juillet-Leclerc and Reynaud,

48 2010). The latter authors show that at 25°C, $\delta^{18}O$ measured on *Acropora* clearly increases due to

49 photosynthesis enhancement accompanying raised light intensity, while the skeleton exhibits

50 noticeable infilling, accompanied by a reduced linear extension (Juillet-Leclerc and Reynaud, 2010).

51 In addition, temperature increase is also responsible for photosynthesis enhancement (Juillet-Leclerc

52 et al., 2014). The comparison of biological measurements, such as net productivity and zooxanthellae

53 density (Juillet-Leclerc et al., 2014) highlights the evidence, well known by biologists, that symbiont

Biogeosciences
Discussions

Open Access

EGU

54   distribution on a coral is not homogeneous, varying with coral genera and coral morphology, ambient

55   vegetation in water column, water column depth and potential adaptations (Porter et al., 1984; Kühl et

56   al., 1995; Karako-Lampert et al., 2004; Iluz and Dubinsky, 2015). Juillet-Leclerc et al. (2014) deduced

57   that light should impact each temperature calibration and should be, likely to a large extent,

58   responsible for the vital effect.

59   In the field, according to location, temperature through the seasonality of precipitation and, in turn,

60   nebulosity, is positively or negatively correlated to irradiation. Therefore, seasonal isotopic amplitude

61   should not only reflect the temperature but the global effect of both temperature and light.

62   Additionally, colonies collected on corals grown in the same location do not receive equivalent

63   irradiation according to the water depth and their environment (Felis et al., 2003) and/or samples are

64   not influenced by similar zooxanthellae density due to coral morphology (Land et al., 1974; Juillet-

65   Leclerc, 2014). Consequently, we supposed that δ^{18}O–temperature calibrations established from

66   seasonal isotopic data are strongly impacted by local seasonality and/or characteristics of each colony.

67   But calibrations based on annual data provided by one coral should not be similarly impacted by light

68   as the seasonal data calculated from monthly samples. In turn, the pure temperature impact on δ^{18}O

69   cannot be quantified. Considering that light impacts coral δ^{18}O, what level of $\delta^{18}O_{Seawater}$ may be

70   included in δ^{18}O determination? Is there a hierarchy between temperature and light influence on δ^{18}O?

71   We intend to illustrate the different light effects on coral isotopic calibration *versus* temperature by

72   using earlier published evidence.

73   The paper is structured as follows. First, we will revisit the dataset of Weber and Woodhead (1972),

74   characterised by the unique sampling mode allowing the comparison of several annual coral genera

75   calibrations. Second, we will compare seasonal calibrations estimated for several *Porites* colonies

76   collected in warm and mediate-temperature water (Linsley et al., 1999; Maier et al., 2004; Quinn and

77   Sampson, 2002). Third, we will show that seasonal and annual δ^{18}O–temperature calibrations are not

78   linearly related (Crowley et al., 1999; Boiseau et al., 1998). Then, understanding that the entanglement

79   of environmental parameters and potential tracers captured in coral skeleton over the time imposes the

80   use of statistical multi-proxy treatment as proposed by Hugues and Amman (2009), we will discuss

81   the ways to circumvent what is hidden behind the blurred term 'vital effect' (Lowenstam and Weiner,

82   1989).

83

2 Weber and Woodhead (1972) paper revisited

2.1. Data series

Data published by Weber and Woodhead (1972), in the following referred to as WW72, remains one

of the most exhaustive coral $\delta^{18}O$ databases, although all the compiled data are not available in the

publication. Our present knowledge may shed new light on the coral $\delta^{18}O$–temperature dependence.

As early as 1951, Urey suspected that physiological processes could affect the $\delta^{18}O$ of calcareous

organisms, leading to values out of isotopic equilibrium with seawater, as shown by $\delta^{18}O$ and $\delta^{13}C$

measured in corals collected from Heron Island (Australia) (Weber and Woodhead, 1970). However,

despite depleted $\delta^{18}O$, these values showed apparent temperature dependence. In order to verify the

coral skeleton's capability to capture temperature, they collected several coral genera spread over

tropical oceans (Fig. 1a). WW72 data were used to establish a formula able to predict past SST

following the isotopic thermometer concept (Urey 1947), expressed as:

$$SST°C = A + B \times \delta^{18}O\ (‰) \qquad \text{Eq. (1)}$$

Annual temperature distribution from 21.2 to 29.3°C was prescribed by the 29 sites spread in the

Pacific Ocean (except for two sites in the Atlantic and Indian oceans) (Fig. 1a). Several specimens of

all the genera present on a site, at most 44 coral genera were collected; for example, 54 specimens of

Acropora were collected on Heron Island (Great Barrier Reef) or 39 *Porites* in the Torres Strait

(between Queensland and Papua New Guinea). Because *Acropora* and *Porites* are ubiquitous genera,

Acropora $\delta^{18}O$ calibration was derived from 835 samples and 421 samples of *Porites*. Derived

calibrations (Fig. 1b) may be considered as statistically significant. In addition, isotopic analyses were

conducted on annual samples, identified by X-ray growth bands, a pair of clear and dark bands

corresponding to the annual growth (Barnes and Lough, 1996).

2.1.1 WW72 calibrations

Biogeosciences
Discussions

Open Access

EGU

5

108   Since the goal of the WW72 study was to verify the relationship between $\delta^{18}O$ and SST to predict SST

109   (Epstein 1951, 1953), they established the calibration of temperature relative to $\delta^{18}O$: PT =

110   'paleotemperature curve' i.e. the temperature expressed according to $\delta^{18}O_{carbonate}$ or as reported in

111   Table 4 from the WW72 formula Eq. (1) (Fig. 1b). In this study, the authors neglected the term

112   $\delta^{18}O_{seawater}$. However, in 1972, the annual instrumental temperature precision was much greater than

113   $\delta^{18}O_{carbonate}$ measurement precision. To date, our purpose is not to prove the existence of an isotopic

114   thermometer but rather to check the reliability of the relationship between δ18Ocarbonate and SST.

115   Therefore, we calculated the relationship:

116   $$\delta^{18}O_{carbonate} = a \times SST\ (°C) + b \qquad \text{Eq. (2)}$$

117   where a and b are constants (Fig. 1c), considering that the variable is SST.

118   We are aware that by inverting (1) into (2), from the same dataset, the obtained relationship has not

119   equivalent significance and similar errors in the constants than the relationship calculated from

120   initially published calibrations.

121

122   *2.1.2 Calibrations including $\delta^{18}O_{seawater}$*

123   The WW72 dataset does not take into account δ18Oseawater. Juillet-Leclerc and Schmidt (2001) included

124   annual $\delta^{18}O_{SeaWater}$ values assessed in the calibration established for *Porites* following the formula:

125   $$\delta^{18}O_{carbonate} - \delta^{18}O_{seawater} = \alpha \times SST(°C) + \beta \qquad \text{Eq. (3)}$$

126   where α and β are constants. They obtained:

127   $$\delta^{18}O_{carbonate} - \delta^{18}O_{seawater} = -0.20 \times SST(°C) + 0.45 \qquad \text{Eq. (4)}$$

128   with $R^2 = 0.83$, N = 22, $p < 0.001$, only significant over the SST range from 24 to 30 °C (Juillet-

129   Leclerc and Schmidt, 2001), by introducing δ18Oseawater following two estimates (Fig. 2). The

130   correlation linking $\delta^{18}O$ directly to temperature showed a higher coefficient:

131   $$\delta^{18}O_{carbonate} = -0.27 \times SST(°C) + 2.24 \qquad \text{Eq. (5)}$$

132   with $R^2 = 0.91$, N = 24, $p < 0.001$ (Fig. 1c) including the lowest temperatures neglected in Eq. (4)

133   (Juillet-Leclerc and Schmidt, 2001).

Biogeosciences

Discussions

Open Access

EGU

134   A similar procedure was conducted for *Acropora*, using the same $\delta^{18}O_{seawater}$ estimates. We obtained:

135                     $\delta^{18}O_{carbonate} - \delta^{18}O_{seawater} = -0.21 \times SST\,(°C) + 1.26$ Eq. (6)

136   with $R^2 = 0.87$, $N = 24$, $p < 0.001$ significant over the temperature range from 21 to 30 °C (Fig. 2). In

137   contrast, *Porites* isotopic values associated to the lowest temperatures are included in the calibration.

138   The correlation linking $\delta^{18}O$ and temperature showed a higher coefficient:

139                          $\delta^{18}O_{carbonate} = -0.28 \times SST(°C) + 3.36$ Eq. (7)

140   with $R^2 = 0.97$, $N = 24$, $p < 0.001$ (Fig. 2).

141   Slopes (a) shown by *Porites* and *Acropora* temperature calibrations including $\delta^{18}O_{seawater}$, −0.20 and −

142   0.21‰/°C respectively differ from those deriving only from $\delta^{18}O_{carbonate}$ and temperature. They are

143   close to the slope of −0.19 ‰/°C assessed for inorganic aragonite calibration (Kim et al., 2007).

144   Slopes have been obtained from other genera such as *Platygira*, *Montipora* or *Pavona* (Fig. 2) in

145   different temperature ranges and with variable correlation coefficients. The number of analysed

146   specimens is reduced compared to *Acropora* or *Porites* calibrations (WW72).

147

148   *2.1.3 Relationship between a and b*

149   When comparing constants (a) and (b) from equation (2) for all the genera annual $\delta^{18}O$ *versus* annual

150   temperature of theWW72 data series, we obtained a strongly significant linear relationship:

151                                $b = -27.9a - 5.13$ Eq. (8)

152   with $R^2 = 0.95$, $N = 29$ and $p < 0.001$. We verified that after neglecting extreme values of (b), the

153   relationship remained significant ($R^2 = 0.90$, $N = 26$ and $p < 0.001$) (Fig. 3a). Such a relationship is not

154   hazardous, but reflects inherent features of annual coral $\delta^{18}O$–annual temperature calibrations.

155   We observed in Fig. 1c that some curves converged, defining several bundles. All the groups, formed

156   by genera gathered in the same bundle, are listed in Table 1. In Fig. 1d, we underline that, for example

157   for *Acropora* and *Porites* groups, the convergence corresponds to quantified temperature and isotopic

158   value ranges. When comparing constants of calibrations corresponding to a group, we obtained linear

159   relationships, all showing highly significant correlation coefficients: $R^2 = 0.99$ (Fig. 3b).

160

161   **2.2 Improved meaning of annual calibration from WW72**

162   Each temperature value, corresponding to one island, is associated to the averaged $\delta^{18}O$ measured for

163   corals of the same species, all receiving identical local irradiation. However, several colonies of a

164   same genus might be subjected to different light incidence, intensity depending to relative growth

165   depth, or corals included in the same local environmental could have morphological portion

166   containing higher or lower zooxanthellae distribution or potential adaptation (Porter et al., 1984; Kühl

167   et al., 1995; Karako-Lampert et al., 2004; Iluz and Dubinsky, 2015). WW72 data corresponding to

168   each temperature correspond to colonies numerous enough to represent a quasi-homogenous

169   irradiation. This explains that calibrations assessed for all genera may be significantly compared

170   without taking into account light conditions (Fig. 1). Only these conditions allow the comparison of

171   calibrations assessed for several coral genera.

172

173   *2.2.1 Temperature dependence of coral $\delta^{18}O$*

174   2.2.1.1 Temperature recorded at least twice

175    $\delta^{18}O$ temperature dependence expressed as Eq. (2) stresses the strong temperature effect on isotopic

176   fractionation but this formula excludes $\delta^{18}O_{seawater}$ displayed in the classical thermodynamic expression

177   Eq. (6). After introducing $\delta^{18}O_{seawater}$ into WW72 data, for some genera, *Porites* and *Acropora* genera

178   (Fig. 2)*,* we observed that the usual thermodynamic equation is also significant but to a lower degree;

179   for example by taking into account only temperature, $R^2 = 0.91$ and 0.98 instead of $R^2 = 0.87$ and 0.93

180   for *Porites* and *Acropora* respectively, for the usual thermodynamic equation.

181   In the calibrations depending only on temperature, temperature may act first, according to

182   thermodynamic law (Epstein et al., 1953; Juillet-Leclerc et al., 2014) and second, through the

183   photosynthetic process (Juillet-Leclerc and Reynaud, 2010), which is enhanced by a temperature

184   increase. However, an increase in temperature induces a decrease in $\delta^{18}O$ following the first process

185   while the second mechanism causes a rise in $\delta^{18}O$ confusing the global isotopic effect. Temperature

186   influences $\delta^{18}O$ twice, explaining that temperature is the main factor on isotopic value determination,

187   which does not exclude the role of $\delta^{18}O_{seawater}$.

Biogeosciences
Discussions

8

188

189   2.2.1.2 Annual coral $\delta^{18}O$ contains $\delta^{18}O_{seawater}$

190   Calibrations taking into account $\delta^{18}O_{seawater}$ exhibit a slope value close to that calculated for isotopic

191   equilibrium of inorganic aragonite with water, suggesting that under quasi-uniform light, the isotopic

192   offset of coral $\delta^{18}O$ (the difference between coral $\delta^{18}O$ and value at isotopic equilibrium) is constant,

193   regardless of temperature (Fig. 2).

194   Calibration deduced for *Porites* is restricted to temperatures higher than 25°C, $\delta^{18}O$ corresponding to

195   lowest temperatures being too high to be included on the strongly significant linear curve. For the

196   other genera, n is limited by the lack of these coral colonies on numerous islands.

197   Equations (4) and (6) confirm that, to a lesser degree than temperature, $\delta^{18}O_{seawater}$ may be included

198   in annual coral skeleton $\delta^{18}O$.

199

200   *2.2.2 Relationship between constants a and b*

201   WW72 data reveal a strong relationship between annual $\delta^{18}O$–annual temperature calibrations and

202   taxonomy because each genus shows a unique relationship. Calibration bundles defining groups

203   (Table 1) enhance this feature. Coral genera classification or taxonomy is based on coral morphology.

204   Land et al. (1975) stressed the high $\delta^{18}O$ variability following the longitudinal section on the calices of

205   *Eusmilia fastigiata* or the septa dentations of *Scolymia cubensis* inducing coral skeleton isotopic

206   variations. The authors observed that according to coral location some skeleton portions might be

207   more or less developed, implying a large isotopic variability.

208

209   Considering the relationship $\delta^{18}O_{carbonate} = a \times SST$ (°C) $+ b$ Eq. (2) derived from the WW72 dataset,

210   (a), the slope value, varies from –0.16 to –0.36. This corresponds to a disequilibrium indicator

211   compared to –0.19, the slope value derived from the theoretical $\delta^{18}O$–temperature equation at

212   equilibrium (Kim et al., 2007). The equation (7) exhibits that the constants (a) and (b) of annual $\delta^{18}O$–

213   annual temperature calibrations established for several annual samples collected from all WW72 coral

214   genera, obey to a linear relationship (Fig. 3): $b = -29.07 \times a - 5.13$ Eq. (8) with N = 37 and $R^2 = 0.95$,

215   p<0.001. This suggests that the temperature dependence of isotopic oxygen ratio is based on a unique

216   rationale according to taxonomy, inherent to the coral skeleton.

217

218   2.2.2.1 Common feature of $\delta^{18}O$ and Sr/Ca calibrations

219   A similar relationship exists between the constants of annual coral skeleton Sr/Ca–annual temperature

220   calibration (Marshall and McCulloch, 2002; Wei et al., 2007; Deng et al., 2014; D'Olivio et al., 2018),

221   another temperature tracer present in the coral skeleton. There is no straightforward link between $\delta^{18}O$,

222   oxygen being a component of CaCO3 and Sr, an impurity included in the skeletal aragonite. However,

223   it is possible to recognise common $\delta^{18}O$ and Sr/Ca behaviour relative to their crystalline unit

224   distribution in the coral skeleton and the concept of taxonomy.

225

226   2.2.2.2 Role of crystalline microstructures

227   It is admitted that the coral skeleton presents composite mineral microstructures: centres of

228   calcification (COC) and fibres, embedded in a few organic matter as a network (Von Euw et al.,

229   2017). These crystalline elements are distributed differently according to morphology (Cuif and

230   Dauphin, 1978, 2005; Stolarski, 2003; Nothdurft and Webb, 2005). The latter authors showed that

231   each microstructure is preferentially present in some morphological parts, which are more or less

232   developed following the genus. On one hand, $\delta^{18}O$ signature differs according to the microstructure

233   unit (Rollion-Bard et al., 2003; Blamart et al., 2005; Meibom et al., 2006; Juillet-Leclerc et al., 2009),

234   the COC $\delta^{18}O$ value being lower than that of the fibre. On the other hand, Sr/Ca ratios measured on

235   COCs are higher than those of fibres (Meibom et al., 2006; Cohen et al., 2001). Meibom et al. (2006)

236   sampled *Colpophyllia sp.* following microstructures on a skeleton morphology fragment and their

237   Sr/Ca data of each crystal type show convergence. Cohen et al. (2001) examined synchronously

238   deposited microstructures on *Porites lutea* over a year, exhibiting COC elemental ratios systematically

239   higher compared to those of fibres developed over an identical period. Thus, the annual COC Sr/Ca

240   value is higher than the annual fibre Sr/Ca signature (Cohen et al., 2001). Therefore, we suggest that

241   discrepancies of morphology existing between coral genera are due to differences of microstructure

242 proportions. Therefore, differences in geochemical values due to the relative number of

243 microstructures could explain common features between the annual trace element ratio and annual

244 δ^{18}O–annual temperature calibrations, especially the linear relationship linking the respective

245 calibration constants.

246

247 *2.2.3 Notion of optimal growth*

248 We already identified groups of genera (Table 1) showing constants (a) and (b) from calibrations of

249 genera linked by strong correlation coefficient ($R^2 = 0.99$) (Fig. 3b). This could be due to morphology

250 similarities of the genera of each bundle, characterised by identical proportions of microstructures in

251 each coral group skeleton. We previously highlighted the intersection of calibrations defined by

252 coupled $SST_{intersection}$ and $\delta^{18}O_{intersection}$, independently to $\delta^{18}O_{seawater}$ (Fig. 3b). Such a common isotopic

253 composition can be obtained because light intensity is homogenised. Coupled values ($SST_{intersection}$ and

254 $\delta^{18}O_{intersection}$) might be related to the concept of the optimal growth conditions (Jokiel and Coles, 1977)

255 attributed to an optimal growth temperature.

256 An optimal temperature, between 25 and 29°C, corresponding to an optimal growth rate has been

257 attributed to some coral genera, *Montipora verrucosa*, *Pocillopora damicormis*, *Fungia scutaria*

258 (Jokiel and Coles, 1977). However, it was difficult to identify a temperature value corresponding to

259 optimal growth conditions: is maximal extension rate or density considered as representative of

260 optimal growth rate (Carricart–Ganivet et al., 2004; Worum et al., 2007; Brachert at al., 2013)? This

261 concept could also be linked to the temperature corresponding to the maximal Ca^{2+} input in the coral

262 skeleton, as has been identified by Al-Horani (2005). Optimal growth temperature differs according to

263 coral genus (Buddemeier and Kinzie III, 1976; Marshall and Clode, 2004). The latter authors relate the

264 temperature dependence of the optimal growth rate of *Galaxea facsicularis* to an enzyme-catalysed

265 reaction, but they finally conclude that the response of calcification rate to temperature being similar

266 in zooxanthellate and azooxanthellate corals, the responsible mechanism should be based on another

267 fundamental process. After studying the calcification of 38 *Porites* colonies, Cooper et al. (2008)

11

268   suggest that 26.7°C could be the thermal optimum of calcification rate for this genus, which could be

269   compared with our $SST_{intersection}$ identified for *Porites*, of 28.4°C.

270   From our evidence, $SST_{intersection}$ corresponds to $\delta^{18}O_{intersection}$ shared by a coral group and is related to

271   morphology and growth rate (Land et al., 1975), likely related to optimal growth. Assuming that

272   relative amounts of crystalline units are responsible for the constant relationship of the annual $\delta^{18}O$–

273   annual temperature calibration, we have to assume that at this temperature, identical $\delta^{18}O$ is due to the

274   same relative crystalline amounts in the coral skeleton, whatever is the considered genus belonging to

275   the same group (Table 1) or, more probably, a temperature range corresponding to an isotopic range

276   (Fig. 1d). For example, the coupled $SST_{intersection}$ and $\delta^{18}O_{intersection}$ could represent common values

277   shared by all *Acropora* or *Porites* colonies whatever is the site where they grow (Fig. 3).

278

279   The following conclusions concern all coral genera studied in WW72 and their annual $\delta^{18}O$–

280   calibrations. Temperature prevails on $\delta^{18}O$ because it influences $\delta^{18}O$ in two ways, first it acts as is

281   thermodynamically predicted, implying a $\delta^{18}O$ decrease and second it induces an enhancement of

282   photosynthesis causing a $\delta^{18}O$ increase. Similar behaviour of the constants of the annual $\delta^{18}O$ and

283   Sr/Ca–annual temperature calibrations should be explained by the presence of two crystallographic

284   components of the coral skeleton, showing specific COC–to–fibre proportions for each genus,

285   depending on their morphology and characterised by their respective geochemical signatures.

286   We deduce from WW72 data that all the coral genera are potential temperature tracers.

287   It is possible to associate to each genus (likely to each bundle) a temperature range coupled to a $\delta^{18}O$

288   range corresponding to optimal growth rate.

289

290   **3 *Porites* monthly calibration**

291   The first seasonal $\delta^{18}O$ records were measured for *Montastrea annularis* (Fairbanks and Dodge,

292   1979). Seasonal $\delta^{18}O$ profiles from *Porites* grown in the Galapagos (McConnaughey, 1989) were used

Biogeosciences

Discussions

EGU

Open Access

12

293   to assess seasonal δ^{18}O–seasonal temperature calibration. Presently, such a regression is commonly

294   calculated.

295   The preliminary step of climatic reconstruction using *Porites* skeleton, the genus more often analysed

296   in this context, consists of the assessment of seasonal δ^{18}O–seasonal temperature calibration based on

297   monthly instrumental temperatures over the last decades covered by the core. Sampling is conducted

298   along the coral's growth through time, following the maximal growth rate perpendicular to the annual

299   density bands shown by X-ray (DeLong et al., 2013).

300   In order to test seasonal δ^{18}O–seasonal temperature calibration variability including the seasonal light

301   effect, calculated for several coral cores collected on a given site, at different temperature ranges, we

302   considered studies conducted on several *Porites* colonies from three sites. The mean annual

303   temperature offshore Amédée Island, New Caledonia (22° 29' S, 166° 28' E) was 24.72°C, over the

304   period 1968–1992 (Quinn and Sampson, 2002; Stephans et al., 2004), while at Clipperton Atoll (10°

305   18' N, 109° 13' W) the mean annual temperature was 28.5°C, over the period 1985–1995 (Linsley et

306   al., 1999, 2000) and in the Flores Sea, Indonesia (6° 32' S, 121° 13' E) the mean annual temperature

307   was above 28°C, over the period 1979–1985 (Maier et al., 2004).

308

3.1 Data in the three sites

3.1.1 Calibrations from New Caledonia data

311   Calibrations have been calculated for two paths of a long core 92 and 99-PAA and two short cores 92-

312   PAC and 92-PAD, collected from *Porites lutea*, compared to the appropriate grid square GISST2

313   temperature from 1968 to 1992 (Quinn and Sampson, 2002; Stephans et al., 2004). These data are

314   available on https://www.ncdc.noaa.gov/paleo/study/1877. Seasonal temperature varied from 21.5 to

315   27.5°C, values lower than the SST$_{intersection}$ estimated for *Porites*, of 28.4°C. Precipitation did not show

316   any preferential seasonality. The δ^{18}O record from all the cores displayed a clear seasonal cycle

317   (Quinn and Sampson, 2002; Stephans et al., 2004). All the calibrations given following Eq. (2)

318   showed higher slope than –0.19, the slope value derived from the theoretical δ^{18}O–

319   temperature relationship at equilibrium (Kim et al., 2007), and varying, comprised between –0.13 and

13

320   –0.17 (Fig. 4a, 4b). When comparing (a) and (b) from the calibrations, a strongly correlated

321   relationship is obtained (Table 2) (Fig. 4c).

322

323   *3.1.2 Calibration from Clipperton Atoll data*

324   We considered three *Porites* cores (Linsley et al., 1999; 2000) whose data are provided on

325   https://www.ncdc.noaa.gov/paleo/study/1846. Over the last decade, annual temperature varied less

326   than 2 °C (Reynolds and Smith, 1994), showing a mean value of 28.5 °C and a clear seasonal cycle

327   (Linsley et al., 1999; 2000). Maximum lag between $\delta^{18}O$ and temperature is at least 1 month,

328   occasionally up to 2 months (Linsley et al., 1999; 2000).

329   Expressed following Eq. (2), calibrations showed low slopes, compared to –0.19, the slope value

330   derived from the theoretical $\delta^{18}O$–temperature relationship at equilibrium (Kim et al., 2007), varying

331   between –0.4 and –0.53 ‰/°C (Fig. 5a, 5b), (a) and (b) being strongly correlated (Table 2) (Fig. 5c).

332

333   *3.1.3 Calibration from the Flores Sea*

334   Twelve pathways collected on six coral heads from three *Porites* species (*Porites lutea*, *Porites*

335   *murrayensis* and *Porites australiensis*) (Fig. 6a, 6b) provide 12 calibrations given following equation

336   (2) covering 55 months and converted into Eq. (3) (Maier et al, 2004). In the site located at the

337   western margin of the Warm Pool, the mean annual temperature is 28°C with an annual amplitude of

338   2.5°C. Although the assessed constants are known to be not free of errors, the relationship established

339   between (a) and (b) showed a highly significant correlation coefficient (Table 2) (Fig. 6c, 6d). It is

340   noticeable that several *Porites* species were considered.

341   We display together all the *Porites* calibrations previously mentioned in Fig. 7a and equation

342   corresponding to *Porites* group V from WW72, covering high temperature amplitude and

343   disequilibrium indicator range. The values of the constants (a) and (b) of all the calibrations are

344   reported in Fig. 7b. The correlation coefficient of the linear regression is 0.999, N = 25.

345

14

346   **3.2 Significance of the constants of δ^{18}O-temperature calibrations derived from**

347   **monthly data.**

348   We assume that calibrations measured on different coral colonies grown at a given site (New

349   Caledonia, Clipperton or Indonesia) differ according to various light sensitivities due to depth or light

350   incidence or acclimation (Fig. 7a) because seasonality strongly affects light variations, and is likely to

351   be different following site location. However, calibration constants calculated from monthly data for

352   *Porites* remain strongly correlated (Fig. 7b) as we observed for annual δ^{18}O–annual temperature

353   calibrations (2.2.2).

354

355   *3.2.1 Local effects on δ^{18}O*

356   The isotopic characteristics may be explained by local conditions. In New Caledonia the mean annual

357   temperature, 24.72°C, is lower than the temperature intersection estimated for *Porites* group from

358   WW72 (Fig. 4) of 28.4°C, the annual amplitude being 6°C. To justify the weak slope of the

359   calibrations, we argue that maximal annual temperature and high light are synchronous: thus, the δ^{18}O

360   decrease due to temperature being reduced during boreal summer and during winter is normal.

361   Therefore, the annual isotopic amplitude is limited. 92PAC and 99PAA show strong attenuation in

362   boreal summer (Fig. 4a), which could be related to strong photosynthetic activity. However these coral

363   cores also exhibit low δ^{18}O during winter according to lower slopes of calibrations for 92PAC and

364   99PAA compared to 92PAC and 92PAD (Fig. 4b).

365   However, in Clipperton and in Indonesia, the mean annual temperature is about 28°C with a weak

366   annual temperature amplitude (about 2°C). In these conditions, the disequilibrium indicator (a) varies

367   from –0.6 to –0.4 (Fig. 7b). The temperature range in Clipperton and the Flores Sea is close to the

368   temperature intersection estimated for *Porites* group from WW72, at 28.4°C (Fig. 5 and Fig. 6

369   respectively). In Indonesia, slope (a) shows much higher range, from –0.4 to –1 than at Clipperton.

370   Maier et al. (2004) stress that calibrations are calculated from several *Porites* species (Fig. 6). The

371   authors also observe negative correlation between mean annual coral δ^{18}O and annual linear skeletal

372   extension.

373

374   *3.2.2 Correlation of the constants derived for monthly δ^{18}O–temperature calibrations*

375   Relationships calculated from monthly data measured in Indonesia (Fig. 6) and Clipperton (Fig. 5)

376   corals (Maier et al., 2004; Linsley et al., 1999) are almost the same. This could be due to the identical

377   temperature range (from 26 to 29°C). As calibrations do not obey only thermodynamic rules,

378   δ^{18}O$_{seawater}$ is neglected. The relationships linking (a) and (b) do not depend on local environmental

379   parameters and seem to be inherent to *Porites* calcification, as we noticed for annual calibrations

380   (2.2.1.1). Furthermore, calibration constants deduced from New Caledonia corals, subject to

381   drastically different external conditions from in the other sites, follow the same linear relationship

382   (Table 2) (Fig. 7a, b). Moreover, the constants calculated for annual data of *Porites* derived from

383   WW72 are included in the linear relationship (Fig. 7b). The relationship b = –27.24 and a –4.92

384   (established with N = 19, R^2 = 0.999) Eq. (7) (Fig. 7b) reflects *Porites* skeleton crystallisation,

385   regardless of other external conditions, including light.

386   However, we demonstrated that light affected cultured *Acropora* (Juillet-Leclerc and Reynaud, 2010).

387   Is such a behaviour only restricted to *Acropora*? The latter authors attributed this feature to the

388   existence of two distinct crystallisation modes of COC and fibres, which are common to other

389   *Acropora* species (Gladfelter, 1982) but also to other genera (Jell, 1974).

390   Therefore, constants of monthly δ^{18}O–monthly temperature calibrations show a strong relationship

391   (Fig. 7) due to crystalline distribution of the coral skeleton, COCs being fusiform crystals deposited

392   according to temperature, regardless of light intensity, ensuring linear extension whereas fibres

393   formation ensuring infilling is light- and temperature-dependent (Gladfelter, 1982; Juillet-Leclerc and

394   Reynaud, 2010; Juillet-Leclerc et al., 2018). We have already highlighted that the relationship linking

395   constants of annual δ^{18}O–annual temperature calibration is due to the relative numbers of crystalline

396   units present in the coral skeleton, including both temperature-dependent crystals, COC and fibres also

397   light-dependent crystals. By considering Fig.7b, only constants from New Caledonia calibration show

398   slope (a) values higher than –0.19, the slope value derived from the theoretical δ^{18}O–

399   temperature relationship at equilibrium (Kim et al., 2007), corresponding to coral fragments where

Biogeosciences
Discussions

Open Access

EGU

16

400   fibres are in higher numbers than COCs, whereas the other slope values lower than –0.19 correspond

401   to coral portions where COC numbers are higher than fibres.

402   Considering seasons over a year, an increase (decrease) of temperature induces $\delta^{18}O$ decrease

403   (increase), and temperature increase (decrease) induces $\delta^{18}O$ increase (decrease) through

404   photosynthetic increase (decrease) with increasing (decreasing) temperature (Juillet-Leclerc and

405   Reynaud, 2010; Juillet-Leclerc et al., 2014).

406

407   Therefore, for *Porites*, when absolute value of the slope exceeds the absolute value of the quasi-

408   equilibrium a = –0.20 (b = 0.46) obtained from WW72 data, the value of (a) corresponds to numbers

409   of COCs compared to fibres due to high temperature, explaining that coral skeleton $\delta^{18}O$ decreases

410   when coral linear extension increases (Maier et al., 2004).

411   At every temperature, for annual or monthly resolution, regardless of external conditions, the

412   distribution of microstructures creates linear relationships between the constants of calibrations of

413   *Porites*, in turn causing density fluctuations (Gladfelter, 1982; Lough and Cooper, 2011).

414

415   *3.2.3 Role of growth rates*

416   RX images of the cores measured on New Caledonia have been published (DeLong et al., 2013) where

417   we can see the presence of clear annual banding. However, intra-annual variations of density cannot

418   be recognised. Only careful identification of seasonal temperature fluctuations, with the sampling path

419   reported on the RX image, could provide detailed information. But we know that even when the

420   seasonal density variation is high (Buigues and Bessat, 2001; Lough and Cooper, 2011; Lough and

421   Cantin, 2014) we cannot attribute clear seasonality to the density change.

422   DeLong et al. (2013) stress the importance of the orientation of the growth axis, the corallite

423   distribution and also the distance between density bands underlined by X-rays, knowing that a pair of

424   dark and clear layers indicates a year's deposit (Barnes and Lough, 1996). X-rays could provide

425   information about coral growth rates and the density resulting from the interplay of extension and

426   calcification rates (Lough and Barnes, 2000; Lough, 2008). The latter author remarks: "Routine

17

427   examination of coral growth characteristics in conjunction with geochemical analyses of the same

428   material can greatly enhance the environmental information obtained from coral archives. It is now

429   admitted that skeletal density results from the interplay of several factors, especially temperature and

430   light (Tudhope, 1994; Juillet-Leclerc et al., 2006).

431   As early as 1982, Gladfelter assumed that linear extension and infilling are two independent growth

432   rates, an assumption supported by Juillet-Leclerc and Reynaud (2010). The authors demonstrated that

433   each growth rate is related to preferential deposition of microstructures, COCs ensuring linear

434   extension and fibres, infilling. Furthermore, geochemical investigations reveal that crystal isotopic

435   signatures differ (Rollion-Bard et al., 2003; Maier et al., 2004; Blamart et al., 2005; Meibom et al.,

436   2006; Juillet-Leclerc et al., 2009). COC formation should be related to temperature (Gladfelter, 1984)

437   and fibre deposit depends on both temperature and light (Juillet-Leclerc et al., 2018). Therefore,

438   temperature and light changes interplay to determine skeletal isotopic composition.

439   Sampling conducted as it is described in DeLong et al. (2013) includes both COCs and fibres.

440   Changes of relative amounts of microstructure as illustrated by X-rays and their respective $\delta^{18}O$ are

441   determined by their mechanisms of formation, unknown so far (Juillet-Leclerc et al., 2009). Following

442   isotopic laws, the combination of calcification processes and isotopic fractionation could be expressed

443   as:

444    $$\text{measured } \delta^{18}O = [(x_{COC} \times \delta^{18}O_{COC}) + (x_{fibre} \times \delta^{18}O_{fibre})] / (x_{COC} + x_{fibre}) \qquad \text{Eq. (8)}$$

445   where x_{COC} and x_{fibre} are the relative amounts of the crystal microstructures, with $x_{COC} + x_{fibre} = 1$, and

446    $\delta^{18}O_{COC}$ and $\delta^{18}O_{fibre}$ are their isotopic signatures depending on temperature and temperature and light,

447   respectively. This expression is likely to be simplistic but closer to the truth than the thermodynamic

448   formula. Temperature is the prominent factor because included both in the crystal amounts and the

449   isotopic signatures.

450    $SST_{intersection}$ and the corresponding $\delta^{18}O_{intersection}$ should be related to morphology (Land et al., 1975).

451   When using relationship (8), measured $\delta^{18}O = (x_{COC} \times \delta^{18}O_{COC}) + (x_{fibre} \times \delta^{18}O_{fibre})$, the intersection of

452   calibration should be obtained when $\delta^{18}O_{intersection} = (0.50 \times \delta^{18}O_{COC}) + (0.50 \times \delta^{18}O_{fiber})$ or at

453    $SST_{intersection}$, $\delta^{18}O_{intersection} = (\delta^{18}O_{COC} + \delta^{18}O_{fibre})/2$. As long as temperature does not reach $SST_{intersection}$

18

454   more fibres are formed in the coral skeleton and temperature exceeds $SST_{intersection}$, COC are

455   progressively prevailing.

456

457   The relationship linking constants (a) and (b) of monthly $\delta^{18}O$ and temperature seems to be inherent to

458   *Porites* calcification. Slope or (a) ranges between –0.14 to –0.93, surrounding –0.19, the slope value

459   derived from the theoretical $\delta^{18}O$–temperature relationship at equilibrium (Kim et al., 2007).

460   Variability of (a) is essentially due to the opposite isotopic effect of simultaneous temperature and

461   light occurring during the year. Considerations of coral calibrations established from annual and

462   monthly $\delta^{18}O$ and temperature, reveal the robustness of temperature dependence on isotopic

463   composition and also highlight the role of intra-annual aragonite density in $\delta^{18}O$ determination. We

464   conclude that calibrations cannot be explained by simple thermodynamic calculation but need

465   information about calcification processes and microstructure (COC and fibre) isotope signatures,

466   depending on temperature and light.

467

468   4 $\delta^{18}O$ non-linearity over time

469   4.1 Data

470   *4.1.1 New Caledonia*

471   Crowley et al. (1999) highlighted $\delta^{18}O$ non-linearity over time for *Porites* from isotopic data series

472   measured on a core collected at Phare Amédée (New Caledonia) (Quinn et al., 1998), where cores

473   were also collected for calibrations calculated by Stephans et al. (2004) (paragraph 3.1.1) (Fig. 4).

474   Crowley et al. (1999) assessed the seasonal calibration established with four samples per year over 22

475   years. Then, from this calibration, they predicted temperature variations from 1900 until 1992, which

476   they compared with 20th century GISST2 observed temperatures (Parker et al., 1995) following the

477   same resolution. The calibration cannot be validated, predicted temperatures over 1900–1950 being

478   underestimated against observed temperatures. Crowley et al. (1999) noticed that by using annual

479   calibration, the temperature prediction shows better agreement than that derived from monthly

480   calibration.

19

481

482   *4.1.2 Moorea (French Polynesia)*

483   We provided another example, using isotopic data measured on a *Porites* core harvested in Moorea

484   (French Polynesia) (17° 30' S, 149° 50' W) (Boiseau et al., 1998). Fig. 8 illustrates the $\delta^{18}O$ non-

485   linearity in time. On the left side, (Fig. 8a), seasonal measured data are compared with instrumental

486   seawater temperature between 1980 and 1990 (Boiseau et al., 1998). On the right side, (Fig. 8b), over

487   the last century, annual averaged measured data, originated from the same data series than seasonal

488   data, are compared with estimated temperature in the (1°, 1°) grid containing Moorea (Kaplan et al.,

489   1998). The two curves are displayed to obtain the best matching. The isotopic scale of the two isotopic

490   profiles is common, while measured and estimated temperature scales cover 7 °C and 2 °C

491   respectively. There is a mismatch between annual and monthly calibrations given on a unique isotopic

492   scale.

493

494   Evidence underlined by the New Caledonia and Moorea examples must be considered following our

495   new understanding about environmental forcing.

496

497   **4.2 Comparison of annual and monthly $\delta^{18}O$ profiles**

498   The comparison between $\delta^{18}O$ profiles and GISST (Parker et al., 1995) or Kaplan (Kaplan et al., 1998)

499   data sets, derived from statistical assessments, was performed over the last century. Kaplan et al.

500   (1998) compared ship-derived monthly temperature with the coral-based proxy record from Tarawa

501   atoll (Cole et al., 1993). The authors observed great discrepancy between the two curves, coral

502   estimates being difficult to justify.

503

504   *4.2.1 Discrepancy between statistical and coral-derived temperature reconstruction*

505   4.2.1.1 Comparison of annual and monthly calibrations in New Caledonia

506   We previously displayed monthly calibrations established in New Caledonia (3.2.1 and 3.2.2). Slopes

507   (a) calculated by Stephans et al. (2004) (Table 2) are similar or higher in absolute value than the slope

20

508   from δ^{18}O-temperature calibration utilised by Crowley et al. (1999). The slopes (a) of monthly δ^{18}O–

509   monthly temperature calibrations (Table 2) are strongly affected by reduced summer isotopic values

510   corresponding to the highest temperatures, due to the light effect superimposed on the temperature

511   effect. In contrast, the mean annual isotopic value is not affected by light because this factor varies

512   weakly over successive years and in turn δ^{18}O essentially reflects temperature. Consequently, when

513   monthly calibration is applied to predict temperature, the seasonal δ^{18}O being strongly affected by

514   light induces negative temperature calculations, confirming the effect assessed by Crowley et al.,

515   (1999). As mentioned in Crowley et al. (1999), when the annual calibration is taken into account, the

516   prediction of temperature over several decades becomes realistic.

517

518   4.2.1.2 Comparison of annual and monthly calibrations in Moorea

519   We are aware that in Fig. 8, we compare two reconstructions based on different tools. However,

520   trusting our previous conclusions that annual or monthly δ^{18}O is, to a first approximation, a good

521   temperature tracer, Fig. 8 illustrates the inconsistency between seasonal and interannual isotopic data.

522

523   In Fig. 9a, monthly calibration has been calculated from composite signals over nine years (from1980

524   to 1989). Since they derive from composite data, calibration constants (a) and (b) may not be

525   compared with constants from previous relationships (Fig. 7b) (Table 2). In Moorea, where mean

526   annual temperature is 26.8°C, value of slope (a) from monthly calibration (Fig. 9a) is of the same

527   order as that in New Caledonia (Crowley et al., 1999). However, the slope value –0.24 derived from

528   the annual calibration calculated over 33 years (from 1989 to 1956) (Fig. 9b) is lower than the slope

529   calculated by Crowley et al. (1999), of –0.19. At these sites, rainfall and in turn nebulosity is higher in

530   November–January, the period recording maximal potential irradiation and maximal temperature

531   (Boiseau et al., 1998). Despite nebulosity, irradiation affects photosynthetic activity of zooxanthellae

532   (coral symbionts), strengthened by temperature. Since temperature and light have opposite influences

533   on δ^{18}O, the slope of monthly calibrations is reduced. Seasonality strongly influences intra-annual or

534   seasonal isotopic profiles.

535   During the last century, annual irradiation remained roughly constant. However, global warming

536   caused by progressive temperature increase is limited around the tropical belt compared to higher

537   latitudes; however this concept remains a matter of debate (Vecchi and Soden, 2007; Du and Xie,

538   2009; Zhu and Liu, 2009; Deser et al., 2010). Knowing that the weak temperature increase slightly

539   impacts photosynthetic activity (Juillet-Leclerc et al., 2014), the single temperature effect on $\delta^{18}O$ is

540   weakly lower than the calculated effect neglecting light.

541   The estimation of warming during the 20th century deduced from coral monthly calibration, is

542   estimated to be 1.2 °C (Boiseau et al., 1998), which is too high for a site located in a tropical zone,

543   whereas the trend of annual $\delta^{18}O$ corresponding to 0.25 °C derived by Kaplan et al. (1998) seems

544   more realistic.

545

546   When coral $\delta^{18}O$ is analysed seasonally, the isotopic profile shows a strong light effect during a year

547   while two successive years globally do not reflect light change and only weak temperature influence.

548   Therefore, interannual and monthly $\delta^{18}O$–temperature calibrations for *Porites*, at Moorea and Amédée

549   Lighthouse are not linear. It is misleading to plot on the time scale monthly $\delta^{18}O$ superimposed on

550   interannual $\delta^{18}O$ because, both in French Polynesia and New Caledonia, seasonal $\delta^{18}O$ variations are

551   strongly impacted by both temperature and light and annual variability is slightly influenced by light

552   and only temperature dependent. Consequently, the global warming of the 20th century has to be

553   estimated from the annual temperature scale to remain realistic.

554

555   **5 Consequences for temperature reconstructions**

556   From the literature dedicated to coral reconstruction based on geochemistry, several papers highlight

557   the misfit between instrumental temperature and $\delta^{18}O$ (Quinn et al., 2006) and between instrumental

558   temperature and Sr/Ca records (Alibert and McCulloch, 1997; Crowley et al., 1999, 2000; Nurhati et

559   al., 2011). Estimates of global warming during the last century as deduced by temperature

560   reconstructions seem too high for the tropical zone (Damassa et al., 2006; Gorman et al., 2012;

561   Thierney et al., 2015). A mismatch between seasonal and annual records has been recognized without

562   any explanation proposed (Osborn et al., 2013; Abram et al., 2015). The possible influence of cloud

563   cover on proxies is suspected in a few publications (Cahyarini et al., 2014) but is it attributed to

564   precipitation or to weak photosynthesis?

565   From previous evidence arise three main concerns: $\delta^{18}O$ is essentially dependent on temperature

566   according the relationships that include the lack of consistency between the influence of light on

567   monthly and annual calibrations. All reconstructions based on thermodynamic relationships, such as

568   the coupled Sr/Ca–$\delta^{18}O$ method or the concept of pseudo-proxy induces biased conclusions. In

569   addition, confusion between seasonal and annual calibrations causes misleading interpretations.

570

571   **5.1 The coupled Sr/Ca–$\delta^{18}O$ method**

572   Pioneered investigations (McCulloh et al., 1994; Gagan et al., 1998, 2000), Ren et al. (2002) proposed

573   to deconvolve $\delta^{18}O_{seawater}$ by using subseasonal coral $\delta^{18}O$ and Sr/Ca. This treatment is based on the

574   oxygen thermometer (3):

575 $$\delta^{18}O_{carbonate} - \delta^{18}O_{Seawater} = \alpha + \beta \times SST\ (°C) \qquad \text{Eq. (3)}$$

576   α and β being constants, and the Sr/Ca temperature tracer following also linear relationships. The

577   preliminary condition for applying the Ren et al. (2002) method, "Sr/Ca is solely a function of SST"

578   may prevent any estimation (Gischler et al., 2005) or it is not respected (Wu et al., 2013), inducing

579   spurious interpretations. Temperature values are derived from Sr/Ca and $\delta^{18}O$ calibrations assessed

580   locally from the recent period (Mishima et al., 2010; Cahyarini et al., 2016) or from calibrations

581   already published (Quinn et al., 2006; Nurhati et al., 2009). Then, this STT value is introduced into

582   Eq. (3) and $\delta^{18}O_{seawater}$ time series is estimated. This value may be converted into seasurface salinity

583   (SSS) (Felis et al., 2009; Nurhati et al., 2011; Cahyarini et al., 2014).

584   The reliability of this method is discussed for multiple reasons: i) we clearly demonstrate that Eq. (3)

585   does not include light effect, which causes vital effect; ii) Sr/Ca calibration meaning is increasingly

586   matter of debate (Alibert and Kinsley, 2008; Cahyarini et al., 2008; Alpert et al., 2014), and cultures

587   testing influence of light on *Acropora* proxies show that reliable Sr/Ca response should be obtained

588   only under high light intensity (Juillet-Leclerc et al., 2014); iii) when the Sr/Ca and $\delta^{18}O$ temperature

589   calibrations are applied over a long time scale (more than one century), SST conditions may change at

590   times, making use of the method difficult (Linsley et al., 2004, 2006). Conversion of $\delta^{18}O_{seawater}$ into

591   SSS is not always possible, or oceanic advection could confuse SSS reconstruction because the

592   relationship between $\delta^{18}O_{seawater}$ and SSS is not sufficiently constrained because it is not locally

593   estimated (Cahyarini et al., 2014; Quinn et al., 2006; Iijima et al., 2005) or may be biased by an

594   advection (Delcroix et al., 2011).

595

596   Climate reconstructions based on the coupled Sr/Ca–$\delta^{18}O$ method must be considered with a critical

597   eye because of the constraining conditions.

598

599   **5.2 Monthly and interannual calibrations**

600   The consequences of the non-linearity between monthly and annual isotopic data are multiple. The

601   first implication is the impossibility of plotting a monthly $\delta^{18}O$ curve over several decades or centuries

602   following an isotopic scale on one side and a temperature scale on the other (Quinn et al., 1998; Cobb

603   et al., 2003; Abram et al., 2015). A temperature scale deriving from monthly calibration is strongly

604   impacted by the light effect, whereas an isotopic profile based on annual variability is weakly affected

605   by light. Therefore, monthly and interannual calibrations, established from a single data series, exhibit

606   different slopes and monthly and interannual isotopic signals cannot be superimposed. Consequently,

607   global warming recorded over the 20th century has to be quantified following the annual calibration.

608   The warming effect assessed from monthly calibration is always overestimated in terms of

609   temperature (Linsley et al., 2000; Damassa et al., 2006; Tierney et al., 2015).

610   Oceanographers are commonly face to such a concern as with salinity change not occurring on intra-

611   annual timescale but noticeable on interannual one. Thus, they commonly use 25 month Hanning filter

612   to extract the real salinity variability (Gouriou and Delcroix, 2002). From monthly $\delta^{18}O$ profile

613   covering the total coral core record, it is possible to obtain interannual variability by assessing annual

614   isotopic averages or by applying 25 month filter. The sole seasonal isotopic record is then calculated

Biogeosciences

Discussions

Open Access

EGU

615   by removing the interannual variations. After obtaining two time series, it is necessary to statistically

616   treat each of them.

617

618   **5.3 The pseudo-coral concept**

619   First suggested by Thomson et al. (2011), the relationship $\delta^{18}O_{pseudocoral} = a_1 \times SST + a_2 \times SSS$, a_1 and a_2

620   being constants, established for monthly data, presents the advantage of being easily introduced into a

621   GCM model (Linsley et al., 2017). This could be a good tool to simulate coral isotopic proxy.

622   However, we have clearly highlighted that $\delta^{18}O_{seawater}$ is included in the coral skeleton $\delta^{18}O$ but

623     $\delta^{18}O_{seawater}$ and SSS are not always linearly related during times such as in the case of seawater

624   advection (Delcroix et al., 2011; Linsley et al., 2017). Knowing that the coral $\delta^{18}O$ and temperature

625   relationship is not linear, it is difficult to include the pseudo-coral concept in paleo-climatic studies

626   (Gorman et al., 2012; Hereid et al., 2013; Osborn et al., 2013), the latter author noticing 'a mismatch

627   between seasonal and interannual timescales'. The concept of pseudo-coral is abundantly developed in

628   terms of theoretical reconstruction techniques (Emile-Geay et al., 2013a, 2013b; Wang et al., 2014).

629   In order to remedy this deficiency existing in most paleo-climatic studies, Emile-Geay and Tingley

630   (2015) proposed the use of a simple empirical transform (ITS). However, a much more efficient tool is

631   the identification of the cause of the non-linearity. Such behaviour has been already highlighted (Felis

632   et al., 2000; Zhang et al., 2009; Osborne et al., 2013; Abram et al., 2015; Zinke et al., 2014).

633

634   **5.4 Reconstruction of interannual and interdecadal variations by using SSA**

635   **(Singular Spectrum Analysis) or MTM (Multi-Taper Method)**

636   Briefly, after capturing high- and low-frequencies present in the proxies or reconstructed

637   environmental parameters on interannual data sets (mean seasonal cycle removed), SSA decomposes

638   noisy time series into their dominant variance patterns and MTM determines variance spectra and

639   coherency (Vautard et al., 1992). Climatic variability so studied is the ENSO event occurring at

640   interannual time scale and at a lower frequency, ITCZ (Inter-Tropical Convergence Zone) migrations,

641   the PDO (Pacific Decadal Oscillation) or the IOD (Indian Ocean Dipole) and Asian monsoon.

642   When this method is applied to $\delta^{18}O$ profile, it is difficult to separate temperature and/or salinity

643   change (Felis et al., 2000; Osborne et al., 2014; Cahyarini et al., 2014; Linsley et al., 2017) or to

644   estimate the interaction between IOD and Indian monsoon (Abram et al., 2008). The use of

645   sophisticated statistics does not always allow atmospheric and meteorological interactions to be

646   established if real proxy significance is not considered.

647

648   All the methods or concepts highlighted are used abundantly in papers dealing with the reconstruction

649   of the climate context from coral geochemical tracers; however, they do not respond to the constraints

650   we have underlined during our demonstration.

651

6 Conclusions

653   By revisiting several published papers we have highlighted the role of light in $\delta^{18}O$ determination,

654   light so far being an ignored vital effect. Since temperature and light influences are opposite on $\delta^{18}O$,

655   it is easier to neglect light; however, this explains why synchronous $\delta^{18}O$ variability observed in

656   distinct cores, even synchronous $\delta^{18}O$ variability recorded on the same colony, may differ each other.

657   The WW72 data series reveal that the annual averaged measure of oxygen isotopic ratios performed

658   on several coral colonies of a single genus, collected at one site, allow comparison due to homogenous

659   light effects. This allows stronger conclusions. Interpreted with new eyes, we concluded that it is

660   likely that all coral genera $\delta^{18}O$ levels are strongly temperature-dependent and should be used as

661   tracers of environmental parameters.

662   Temperature appears to be the dominant factor in $\delta^{18}O$ levels because it is recorded in two ways: as a

663   thermodynamic forcing causing $\delta^{18}O$ decrease, and as responsible for photosynthesis enhancement

664   inducing $\delta^{18}O$ increase.

665   After observing the relationships linking the constants of annual (Sr/Ca)–temperature calibrations

666   compared to the relationships linking the constants of annual $\delta^{18}O$–temperature calibrations, we

667   deduced that the analogy should be due to relative amounts of two mineral microstructures, COCs and

668   fibres. COCs probably depend only on temperature and fibres depend on both light and temperature.

Biogeosciences
Discussions

Open Access

EGU

26

669   Similar conclusions derive from revisited monthly δ^{18}O–temperature calibrations assessed for *Porites*

670   coral, in three sites characterised by different annual temperatures. We established a robust

671   relationship linking the constants of the respective δ^{18}O–temperature calibrations calculated on

672   multiple *Porites* colonies of different species. Taking into account all *Porites* δ^{18}O–temperature

673   calibration constants, the high correlation coefficient obtained is at least 0.99, underlining the

674   consistency of the calibrations. In addition, this indicates the prominent role of temperature in δ^{18}O

675   levels, acting both thermodynamically and through photosynthetic activity impacted by temperature.

676   We stress that the relative numbers of mineral microstructures also support this argument.

677   We explained how light impact differs according to annual or monthly time scales. Annual δ^{18}O

678   variations are weakly affected by annual light change while monthly variations are strongly affected

679   by seasonal light. Consequently, a δ^{18}O profile derived from monthly resolution results from the

680   superposition of annual variations weakly affected by annual light change and monthly variations

681   strongly impacted by seasonal light fluctuations. When oxygen isotopes are plotted against

682   temperature, the confusion of time scales generates major misleading. For example, global warming

683   recorded over the 20th century derived from a monthly δ^{18}O profile is overestimated.

684

Bibliography

685

686   Abram NJ, Dixon BC, Rosevear MG, Plunkett B, Gagan MK, Hantoro WS, Phipps SJ (2015),

687   Optimized coral reconstructions of the Indian Ocean Dipole: An assessment of location and

688   length considerations, Paleoceanography, 30, 1391–1405, doi:10.1002/2015PA002810.

689   Alibert C, Kinsley L. (2008), A 170-year Sr/Ca and Ba/Ca coral record from the western Pacific warm

690   pool: 1. What can we learn from an unusual coral record?, J. Geophys. Res., 113, C04008,

691   doi:10.1029/2006JC003979.

692   Alibert C, McCulloch MT (1997), Strontium/calcium ratios in modern *Porites* corals from the Great

693   Barrier Reef as a proxy for sea surface temperature: Calibration of the thermometer and

694   monitoring of ENSO. *Paleoceanography* **12** (*3*), 345–363.

695   Al-Horani FA, Ferdelman T, Al-Moghrabi SM, de Beer D (2005), Spatial distribution of calcification

696   and photosynthesis in the scleractinian coral *Galaxea fascicularis*, Coral Reefs, 24, 173–180,

697   DOI 10.1007/s00338-004-0461-3.

698   Alpert AE, Cohen AL, Oppo DW, DeCarlo TM, Gove JM, Young CW (2016), Comparison of

699   equatorial Pacific sea surface temperature variability and trends with Sr/Ca records from

700   multiple corals, Paleoceanography, 31, doi:10.1002/2015PA002897.

701   Bagnato, S., B. K. Linsley, S. S. Howe, G. M. Wellington, and J. Salinger (2005), Coral oxygen

702   isotope records of interdecadal climate variations in the South Pacific Convergence Zone

703   region, Geochem. Geophys. Geosyst., 6, Q06001, doi:10.1029/2004GC000879.

704   Barnes DJ, Lough JM (1996), Coral skeletons: storage and recovery of environmental information,

705   Glob. Change Biol., 2, 569–582.

706   Bishop, C. M. (1995), Neural Networks for Pattern Recognition, 482 pp., Clarendon, Oxford, U. K.

707   Bessat F, Boiseau M, Juillet-Leclerc A, Buigues D, Salvat B (1997), Computerized tomography and

708   oxygen stable isotopic composition of *Porites lutea* skeleton at Mururoa (French Polynesia):

709   application to the study of solar radiation influence on annual coral growth, C.R.Acad.Sciences

710   de la vie, 320, 659-665.

28

711 Bessat F and Buigues D (2001), Two centuries of variation in coral growth in a massive *Porites*

712 colony from Moorea (French Polynesia) : a response of ocean-atmosphere variability from

713 south central Pacific, *Paleogeography, Paleoclimatology, Paleoecology*, 175, 381-392.

714 Blamart D, Rollion-Bard C, Cuif JP, Juillet-Leclerc A, Lutringer A, van Weering TCE, Henriet JP

715 (2005), C and O isotopes in deep-sea coral (*Lophelia pertusa*) related to skeletal microstructure,

716 in Cold-Water Corals and Ecosystems, edited by A. Freiwald and J. M. Roberts, pp. 1005–1020,

717 Springer, Berlin.

718 Boiseau M, Juillet-Leclerc A, Yiou P, Salvat B, Isdale P, Guillaume M (1998), Atmospheric and

719 oceanic evidences of ENSO events in the south central Pacific Ocean from coral stable

720 isotopic records over the past 137 years, Paleoceanography, 13, 671-685.

721 Brachert TC, Reuter M, Krüger S, Böcker A, Lohmann H, Mertz-Kraus R, Fassoulas C (2013),

722 Density banding in corals: barcodes of past and current climate Change, Coral Reefs, 32, 1013–

723 1023, DOI 10.1007/s00338-013-1056-7.

724 Buddemeier RW, Kinzie III RA (1976), Coral Growth, Oceanogr. Mar. Biol. Ann. Rev., 1976, 14,

725 183-225.

726 Cahyarini SY, Pfeiffer M, Timm O, Dullo WC, Schönberg (2008), Reconstructing seawater $\delta^{18}O$ from

727 paired coral δ18O and Sr/Ca ratios: Methods, error analysis and problems, with examples from

728 Tahiti (French Polynesia) and Timor (Indonesia), Geochim. Cosmochim. Acta, 72, 2841–2853.

729 Cahyarini SY, Pfeiffer M, Nurhati IS, Aldrian E, Dullo WC, Hetzinger S (2014), Twentieth century

730 sea surface temperature and salinity variations atTimor inferred from paired coral $\delta^{18}O$ and

731 Sr/Ca measurements, J. Geophys. Res. Oceans, 119, 4593–4604, doi:10.1002/2013JC009594.

732 Cahyarini SY, Zinke J, Troelstra S, Suharsono, Aldrian E, Hoeksema BW (2016) Coral Sr/Ca-based

733 sea surface temperature and air temperature variability from the inshore and offshore corals in

734 the Seribu Islands, Indonesia, Mar.Poll.Bull., 110, 694-700.

735 Cardinal D, Hamelin **B**, Bard E, Pätzold J (2001), Sr/Ca, U/Ca and $\delta^{18}O$ records in recent massive

736 corals from Bermuda: relationships with sea surface temperature, Chem. Geol.*,* 176, 213-233.

737 Carricart–Ganivet JP (2004), Sea surface temperature and the growth of the West Atlantic reef-

29

738   building coral *Montastraea annularis*, J. Exp. Ma. Biol. Ecol., 302, 249– 260.

739 Cobb KM, Charles CD, ChengH, Edwards RL (2003) El Niño/Southern Oscillation and tropical

740   Pacific climate during the last Millennium, Nature, 424, 271- 276.

741 Cohen AL, Layne GD, Hart SR, Lobel PS (2001), Kinetic control of skeletal Sr/Ca in a symbiotic

742   coral: implications for the paleotemperature proxy. Paleoceanography 16 (1), 20–26.

743 Cole JE and Fairbanks RG (1990), The Southern Oscillation recorded in the $\delta^{18}O$ of corals from

744   Tarawa Atoll, Paleoceanography, 5, 669-683.

745 Cole JE, Fairbanks RG, and Shen GT (1993), Recent variability in the Southern Oscillation: Isotopic

746   results from a Tarawa Atoll coral, Science, 260, 1790-1793.

747 Cooper TM, De'ath G, Fabricius KE, Lough JM (2008), Declining coral calcification in massive

748   *Porites* in two nearshore regions of the northern Great Barrier Reef Global Change Biology 14,

749   529–538, doi: 10.1111/j.1365-2486.2007.01520.

750 Crowley TJ, Quinn TM, Hyde TM (1999) Validation of coral temperature calibrations,

751   Paleoceanography, 14, 605-615.

752 Cuif JP, Dauphin Y, (1998), Microstructural and physico-chemical characterisation of centres of

753   calcification in septa of some Scleractinian corals. Pal Zeit 72:257–270.

754 Damassa TD, Cole JE, Barnett HR, Ault TR, McClanahan TR (2006), Enhanced multidecadal climate

755   variability in the seventeenth century from coral isotope records in the western Indian Ocean,

756   Paleoceanography, 21, PA2016, doi:10.1029/2005PA001217.

757 Delcroix T,.Alory G, Cravatte S, Corrège T, McPhadenMJ (2011), A gridded sea surface salinity data

758   set for the tropical Pacific with sample applications (1950-2008), Deep- Sea Res.I, 58, 38-48.

759 DeLong KL, Quinn TM, Taylor FW, Shen CC, Lin K (2013), Improving coral-base paleoclimate

760   reconstructions by replicating 350 years of coral Sr/Ca variations, Palaeogeog., Palaeoclim.,

761   Palaeoecol., 373, 6–24.

762 Deng W, Wei G, McCulloch M, Xie L, Liu Y, Zeng T (2014), Evaluation of annual resolution coral

763   geochemical records as climate proxies in the Great Barrier Reef of Australia, Coral Reefs, 33,

764   965–977, DOI 10.1007/s00338-014-1203-9.

765 Deser C, Phillips AS, Alexander MA (2010), Twentieth century tropical sea surface temperature

766 trends revisited, Geophys. Res. Lett., 37, L10701, doi:10.1029/2010GL043321.

767 D'Olivo J.P., Sinclair D.J., Rankenburg K., McCulloch M.T. (2018) A universal multi-trace element

768 calibration for reconstructing sea surface temperatures from long-lived Porites corals:

769 Removing 'vital-effects'. Geochim. Cosmochim. Acta 239, 109–135.

770 Du Y, Xie SP (2008), Role of atmospheric adjustments in the tropical Indian Ocean warming during

771 the 20th century in climate models, Geophys. Res. Lett., 35, L08712, doi:10.1029

772 /2008GL033631.

773 Emile-Geay J, Cobb KM, Mann ME, Wittenberg AT (2013a) Estimating Central Equatorial Pacific

774 SST Variability over the Past Millennium. Part I: Methodology and Validation, J. Clim., 26,

775 2302-2328.

776 Emile-Geay J, Cobb KM, Mann ME, Wittenberg AT (2013b) Estimating Central Equatorial Pacific

777 SST Variability over the Past Millennium. Part II: Reconstructions and Implications, J. Clim.,

778 26, 2329 2352.

779 Emile-Geay J, Tingley M (2015), Inferring climate variability from nonlinear proxies: application to

780 palaeo-ENSO studies, Clim. Past, 12, 31–50, www.clim-past.net/12/31/2016/ doi:10.5194/cp-

781 12-31.

782 Epstein S, Buchsbaum R, Lowenstam H, Urey HC (1951), carbonate water isotopic temperature scale,

783 Bull. Geol. Soc. Am., v. 62, p. 417.

784 Epstein S, Buchsbaum R, Lowenstam H, Urey HC (1953), Revised carbonate-water isotopic

785 temperature scale, Bull. Geol. Soc. Am., 62,417-425.

786 Fairbanks RG, Evans MN, Rubenstone1 JL, Mortlock RA, Broad K, Moore MD, CharlesCD (1997)

787 Evaluating climate indices and their geochemical proxies measured in corals, Coral Reefs , 16,

788 Suppl.: S93-S100.

789 Fairbanks RG, Dodge RE (1979) Annual periodicity of the $^{18}O/^{16}O$ and $^{13}C/^{12}C$ ratios in the coral

790 *Montastrea annularis,* Geochim. Cosmochim. Acta, 43, 1009-1020.

791 Felis T, Pätzold J, Loya Y, Fine M, Nawar NJ, Wefer G (2000), A coral oxygen isotope record from

792 the northern Red Sea documenting NAO, ENSO and North Pacific teleconnections on Middle

793 East climate variability since the year 1750, Paleoceanography, 15, 679-694.

794   Felis T, Pätzold J, Loya, Y (2003) Mean oxygen-isotope signatures in *Porites sp.* corals: inter-colony

795   variability and correction for extension-rate effects, Coral Reefs 22, 328–336, DOI

796   10.1007/s00338-003-0324-3.

797   Felis1 T, Suzuki A, Kuhnert H, Dima M, Lohmann G, Kawahata H (2009), Subtropical coral reveals

798   abrupt early-twentieth-century freshening in the western North Pacific Ocean, Geology, 37,

799   527-530.

800   Gagan MK, Ayliffe LK, Hopley D, Cali JA, Mortimer GE, Chappell J, McCulloch MT, Head, M.J.,

801   (1998), Temperature and surface-ocean water balance of the mid-Holocene tropical western

802   Pacific, Science, 279, 1014-1018.

803   Gagan MK, Ayliffe LK, Beck JW, Cole JE, Druffel ERM, Dunbar RB, Shrag DP (2000), New views

804   of tropical paleoclimates from corals, Quatern. Sc. Rev., 19, 45-64.

805   Gagan, MK, Dunbar GB, Suzuki A (2012), The effect of skeletal mass accumulation in *Porites* on

806   coral Sr/Ca and δ^{18}O paleothermometry, Paleoceanography, 27, PA1203,

807   doi:10.1029/2011PA002215.

808   Gattuso JP, Allemand D, Frankignoulle M (1999), Photosynthesis and calcification at cellular,

809   organismal and community levels in coral reefs: a review on interactions and control by

810   carbonate chemistry, Amer. Zool, 39, 160-183.

811   Gischler E, Oschmann W (2005) Historical Climate Variation in Belize (Central America) as

812   Recorded in Scleractinian Coral Skeletons, Palaios, 20, 159–174.

813   Gladfelter EH (1982), Skeletal development in *Acropora cervicornis*: I. Patterns of calcium carbonate

814   accretion in the axial corallite, Coral Reefs,1, 45-51.

815   Gladfelter EH (1984), Skeletal development in *Acropora cervicornis*: III. A comparison of monthly

816   rates of linear extension and Calcium Carbonate accretion measured over a year, Coral Reefs, 3,

817   51-57.

818   Goodkin NF, Hughen KA, Cohen AL, Smith SR (2005), Record of Little Ice Age sea surface

819   temperatures at Bermuda using a growth-dependent calibration of coral Sr/Ca,

820   Paleoceanography, 20, PA4016, doi:10.1029/2005PA001140.

821   Goreau TF (1959), The physiology of skeleton formation in coral I: a method for measuring the rate of

822   calcium deposition under different light conditions, Biol. Bull., 116, 59-75.

823   Gorman, MK, Quinn TM, Taylor FG, Partin JW, Cabioch G, Austin Jr. JA, Pelletier B, Ballu V, Maes

824   C, Saustrup S (2012), A coral-based reconstruction of sea surface salinity at Sabine Bank,

825   Vanuatu from 1842 to 2007 CE, Paleoceanography, 27, PA3226, doi:10.1029/2012PA002302.

826   Gouriou Y, and Delcroix T (2002), Seasonal and ENSO variations of sea surface salinity and

827   temperature in the South Pacific Convergence Zone during 1976–2000, J. Geophys. Res.,

828   107(C12), 8011, doi:10.1029/2001JC000830.

829   Hereid KA, Quinn TM, Okumura YM (2013), Assessing spatial variability in El Niño–Southern

830   Oscillation event detection skill using coral geochemistry, Paleoceanography, 28, 14–23,

831   doi:10.1029/2012PA002352.

832   Hughes MK, Ammann CM (2009), The future of the past—an earth system framework for high

833   resolution paleoclimatology: editorial essay, Clim. Change, 94, 247–259, DOI 10.1007/s10584-

834   009-9588-0.

835   Iijima H, Kayanne H, Morimoto M, Abe O (2005), Interannual sea surface salinity changes in the

836   western Pacific from 1954 to 2000 based on coral isotope analysis, Geophys. Res. Lett., 32,

837   L04608, doi:10.1029/2004GL022026.

838   Iluz D, Dubinski D (2015), Coral photobiology : new light on old views. Zoology 118, 71-78.

839   Jell JS (1974), The microstructure of some scleractinian corals. Proc Second Intl Coral Reef Symp.

840   Austr 2:301-320.

841   Jokiel PL, Coles SL (1977), Effects of temperature on the mortality and growth of Hawaiian reef

842   corals. Mar. Biol. 43, 201-208.

843   Juillet-Leclerc A, Schmidt G (2001), A calibration of the oxygen isotope paleothermometer of coral

844   aragonite from *Porites*, Geophysical Research Letter, 28, 4135-4138, 2001.

845   Juillet-Leclerc A, Thiria S, Naveau P, Delcroix T, Le Bec N, Blamart D, Corrège T (2006), SPCZ

846   migration and ENSO events during the 20th century as revealed by climate proxies from a Fiji

847   coral, Geophys. Res. Lett., 33, L17710, doi:10.1029/2006GL025950.

33

848   Juillet-Leclerc A, Reynaud S, Rollion-Bard C, Cuif JP, Dauphin Y, Blamart D, Ferrier-Pagès C,

849   Allemand D (2009), Oxygen isotopic signature of the skeletal microstructures in cultured

850   corals: identification of vital effects. Geochim. Cosmochim. Acta 73, 5320-5332.

851   Juillet-Leclerc A, Reynaud S (2010), Light effects on the isotopic fractionation of skeletal oxygen and

852   carbon in the cultured zooxanthellate coral, *Acropora*: implications for coral-growth rates.

853   Biogeosciences 7, 893–906.

854   Juillet-Leclerc A, Reynaud S, Dissard D, Tisserand G, Ferrier-Pagès C (2014), Light is an active

855   contributor to vital effects of coral skeleton proxies. Geochim. Cosmochim. Acta 140, 671-690.

856   Juillet-Leclerc A, Rollion-Bard C, Reynaud S, Ferrier-Pagès C (2018), A new paradigm for δ18O in

857   coral skeleton oxygen isotope fractionation response to biological kinetic effects, Chem. Geol.,

858   483, 131-140.

859   Karako-Lampert S, Katcoff DJ, Achituv Y, Dubinski Z, Stambler N (2004), Response of

860   Symbiodinium microadriaticum clade B to different environmental conditions. J. Exp. Mar. Bio.

861   Ecol. 318, 31–38.

862   Kaplan A, Cane M, Kusnir Y, Blumenthal B, Rajagopalan B (1998), Analyses of global Sea Surface

863   Temperature 1856-1991, Journal of Geophysical Research, 103, 18567-18589.

864   Kim ST, O'Neil JR, Hilaire-Marcel C, Mucci A (2007), Oxygen isotope fractionation between

865   synthetic aragonite and water. Influence of temperature and Mg^{2+} concentration. Geochim.

866   Cosmochim. Acta 71, 4704-4715.

867   Kühl M, Cohen Y, Dansgaard T, Jorgensen BB, Revsbech NP (1995), Microenvironmental and

868   photosynthesis in scleractininan corals studied with microsensors for O_2, pH and light. Marine

869   Ecology Progress Series 117, 159-172.

870   Land LS, Lang JC, Barnes DJ (1975), Extension rate: a primary control on the isotopic composition of

871   west Indian (Jamaican) scleractinian reef coral skeletons, Mar. Biol. 33, 221-233.

872   Le Bec N, Juillet-Leclerc A, Correge T, Blamart D, Delcroix T (2000), A coral $\delta^{18}O$ record of ENSO

873   driven sea surface salinity in Fiji (south-western tropical Pacific), Geophys. Res. Lett. 27, 3897-

874   3900.

34

875   Linsley BK, Messier RG, Dunbar RB (1999), Assessing between-colony oxygen isotope variability in

876   the coral *Porites lobata* at Clipperton Atoll, Coral Reefs, 18, 13-27.

877   Linsley BK, Wellington GM, Schrag GM (2000), Decadal Sea Surface Temperature Variability in the

878   Subtropical South Pacific from 1726 to 1997 A.D. Science 290, 1145-1148.

879   Linsley BK, Wellington GM, Schrag DP, Ren L, Salinger MJ, and Tudhope AW (2004), Geochemical

880   evidence from corals for changes in the amplitude and spatial pattern of South Pacific

881   interdecadal climate variability over the last 300 years, Clim. Dyn., 22, 1–11, doi:10.1007/

882   50038200 -0364-y.

883   Linsley BK, Kaplan A, Gouriou Y, Salinger J, deMenocal PB, Wellinton GM, Howe SS (2006),

884   Tracking the extent of the South Pacific Convergence Zone since the early 1600s, Geochem.,

885   Geophys. Geosys. 7 doi:10.1029/2005GC001115.

886   Linsley,B K, Wu HC, Rixen T, Charles CD, $ Gordon AL, Moore MD (2017), SPCZ zonal events and

887   downstream influence on surface ocean conditions in the Indonesian Throughflow region,

888   Geophys. Res. Lett., 44, 293–303, doi:10.1002/2016GL070985.

889   Liu Y, Peng Z, Shen CC, Zhou R, Song S, Shi Z, Chen T, Wei G, DeLong KL (2013), Recent 121-

890   year variability of western boundary upwelling in the northern South China Sea, Geophys. Res.

891   Lett., 40, 3180–3183, doi:10.1002/grl.50381.

892   Lough JM, Barnes DJ (2000), Environmental control on growth of the massive coral *Porites,* J. Exp.

893   Mar. Biol. Ecol., 245, 225-43.

894   Lough, JM (2008), Shifting climate zones for Australia's tropical marine ecosystems, Geophys. Res.

895   Lett., 35, L14708, doi:10.1029/2008GL034634.

896   Lough JM, Cooper TF (2011), New insights from coral growth band studies in an era of rapid

897   environmental change, Earth-Science Reviews, 108, 170–184.

898   Lough JM, Cantin NE (2014), Perspectives on Massive Coral Growth Rates in a Changing Ocean,

899   Biol. Bull. 226: 187–202.

900   Lowenstam HA, Weiner S (1989), On Biomineralization. Oxford University Press, New York p 207-

901   251.

902 McConnaughey TA (1989), C-13 and O-18 isotopic desequilibrium in biological carbonates: I.
903   Patterns. Geochim. Cosmochim. Acta 53, 151-162.

904 McCulloch, MT, Gagan MK, Mortimer GE, Chivas AR, Isdale PJ (1994), A high-resolution Sr/Ca and
905   δ^{18}O coral record from the Great Barrier Reef, Australia, and the 1982-1983 El Niño, Geochim.
906   Cosmochim. Acta, 5c8, 2747-2754.

907 Maier C, Felis T, Pätzold J, Bak RPM (2004), Effect of skeletal growth and lack of species effects in
908   the skeletal oxygen isotope climate signal within the coral genus Porites, Marine Geology, 207,
909   193– 208.

910 Marshall JF, McCulloch MT (2002), An assessment of the Sr/Ca ratio on shallow water hermatypic
911   corals as a proxy for sea surface temperature. Geochim. Cosmochim. Acta **66**, 3263–3280.

912 Marshall AT, Clode P (2004), Calcification rate and the effect of temperature in a zooxanthellate and
913   an azooxanthellate scleractinian reef coral, Coral Reefs 23, 218–224, DOI 10.1007/s00338-004-
914   0369-y.

915 Meibom A, Yurimoto H, Cuif JP, Domart-Coulon I, Houlbrèque F, Constantz B, Dauphin Y,
916   Tambutté E, Tambutté S, Allemand D, Wooden J, Dunbar R, (2006), Vital effect in coral
917   skeletal composition display strict three-dimensional control, Geophys. Res. Let. 30, doi:10,
918   1029/2006GL025968.

919 Mishima M, Suzuki A, Nagao M, Ishimura T, Inoue M, Kawahata H (2010), Abrupt shift toward
920   cooler condition in the earliest 20th century detected in a 165 year coral record from Ishigaki
921   Island, southwestern Japan, Geophys. Res. Lett., 37, L15609, doi:10.1029/2010GL043451.

922 Nothdurft LD, Webb GE (2007), Microstructure of common reef-building coral genera *Acropora*,
923   *Pocillopora*, *Goniastrea* and *Porites*: constraints on spatial resolution in geochemical sampling,
924   Facies, 53, 1-26.

925 Nurhati, I. S., K. M. Cobb, C. D. Charles, and R. B. Dunbar (2009), Late 20th century warming and
926   freshening in the central tropical Pacific, Geophys. Res. Lett., 36, L21606,
927   doi:10.1029/2009GL040270.

928 Nurhati I.S., Cobb K.M. and Di Lorenzo E. (2011) Decadal-Scale SST and Salinity Variations in the
929   Central Tropical Pacific: Signatures of natural and anthropogenic climate change, J. Clim. 24,

36

930   3294-3308, DOI: 10.1175/2011JCLI3852.

931   Osborne MC, Dunbar RB, Mucciarone DA, Sanchez-Cabeza JA, Druffel H (2013), Regional

932   calibration of coral-based climate reconstructions from Palau, West Pacific Warm Pool

933   (WPWP), Palaeogeog. Palaeoclim. Palaeoecol., 386, 308–320.

934   Osborne MC, Dunbar RB, Mucciarone DA, Druffel H, Sanchez-Cabeza JA (2014), A 215-yr coral

935      $\delta^{18}O$ time series from Palau records dynamics of the West Pacific Warm Pool following the

936   end of the Little Ice Age, Coral Reefs, 33, 719–731 DOI 10.1007/s00338-014-1146-1.

937   Parker DE, Folland CK, Jackson M (1995), Marine surface temperature: observed variations and data

938   requirements, Clim. Change, 31, 559-600.

939   Porter JW, Muscatine L, Dubinski Z, Falkowski PG (1984), Primary production and photoadaptation

940   in light- and shade-adapted colonies of the symbiotic corals *Stylophora pistillata*, Proc. R. Soc.

941   Lond. B 222, 161–180.

942   Quinn TM, Crowley TJ, Taylor FW, Hénin C, Joannot P, Join Y (1998), A multicentury isotope

943   record from a New Caledonia coral: interannual and decadal sea surface temperature variability

944   in the southwest Pacific since 1657 A.D., Paleoceanography, 13, 412-426.

945   Quinn TM, Sampson DE (2002), A multiproxy approach to reconstructing sea surface conditions

946   using coral skeleton geochemistry, Paleoceanography, 17, 1062, doi:10.1029/2000PA000528.

947   Quinn,TM, Taylor FW, Crowley TJ (2006), Coral-based climate variability in the Western Pacific

948   Warm Pool since 1867, J. Geophys. Res., 111, C11006, doi:10.1029/2005JC003243.

949   Ren L, Linsley BK, Wellington GM, Schrag DP, Hoegh-Guldberg O (2003), Deconvolving the $\delta^{18}O$

950   seawater component from subseasonal coral $\delta^{18}O$ and Sr/Ca at Rarotonga in the southwestern

951   subtropical Pacific for the period 1726 to 1997, Geochim. Cosmochim. Acta, 67, 1609-1621.

952   Reynaud-Vaganay S, Juillet-Leclerc A, Gattuso JP, Jaubert J (2001), Effect of light on skeletal $\delta^{13}C$

953   and $\delta^{18}O$ and interaction with photosynthesis, respiration and calcification in two

954   zooxanthellate scleractinian corals, Paleogeogr., Paleoclim., Paleoecol., 175, 393-404.

955   Reynaud-Vaganay S, Ferrier-Pagès C, Sambrotto R, Juillet-Leclerc A, Jaubert J, Gattuso JP (2002), A

956   novel culture technique for scleractinian corals: application to investigate changes in skeletal

957         $\delta^{18}O$ as a function of temperature, Mar. Ecol. Prog. Series, Vol. 238: 81–89.

958   Reynolds RW, Smith TM (1994), Improved global sea surface temperature analysis using optimum

959   interpolation, J. Clim, 7, 929-948.

960   Rollion-Bard C, Chaussidon M, France-Lanord C (2003), pH control on oxygen isotopic composition

961   of symbiotic corals, Earth and Planetary Science Review, 215, 265-273.

962   Stephans CL, Quinn TM, Taylor FW and Corrège T (2004) Assessing the reproducibility of coral-

963   based climate records, Geophys. Res. Lett., 31, L18210, doi:10.1029/2004GL020343.

964   Stolarski J (2003), Three-dimensional micro- and nanostructural characteristicsof the scleractinian

965   coral skeleton: a biocalcification proxy, Acta Palaeontol Polonica, 48, 497–530.

966   Su H, Jiang JH, Vane DG, Stephens GL(2008), Observed vertical structure of tropical oceanic clouds

967   sorted in large-scale regimes, Geophys. Res. Lett., 35, L24704, doi:10.1029/2008GL035888.

968   Thompson, D. M., T. R. Ault, M. N. Evans, J. E. Cole, and J. Emile‑Geay (2011), Comparison of

969   observed and simulated tropical climate trends using a forward model of coral $\delta^{18}O$, Geophys.

970   Res. Lett., 38, L14706, doi:10.1029/2011GL048224.

971   Tierney, JE, Abram NJ, Anchukaitis KJ, Evans MN, Giry C, Kilbourne KH, Saenger CP, Wu HC,

972   ZinkeJ (2015), Tropical sea surface temperatures for the past four centuries reconstructed from

973   coral archives, Paleoceanography, 30, doi:10.1002/2014PA002717.

974   Tudhope AW, Shimmield GB, Chilcott CP, Jebb M, Fallick AE, Dalgleish AN (1995), Recent

975   changes in climate in the far western equatorial Pacific and their relationship to the Southern

976   Oscillation: Oxygen isotope records from massive corals, Earth and Planetary Science Letters,

977   136, 575-590.

978   Urey HC, Thermodynamic properties of isotopic substances, *Jour. Chem. Soc.*, 562-581, 1947.

979   Urey HC, Lowenstam HA, Epstein S, McKinney CR (1951), Measurements of paleotherperature of the upper

980   cretaceous of England, Denmark, and the Southeastern United States, Bull. Geol. Soc. Am., 62, 399-416.

981   Vautard R, Yiou P, Ghil M (1992), Singular-spectrum analysis: A toolkit for short, noisy chaotic

982   signals, Phys. D, 58, 95-126.

983   Vecchi GA, Soden BJ (2007), Global Warming and the Weakening of the Tropical Circulation, J.

984   Clim. 20, 4316-4340, DOI: 10.1175/JCLI4258.1.

985   Von Euw S, Zhang Q, Manichev V, Murali N, Gross J, Feldman LC, Gustafsson T, Flach C,

986   Mendelsohn R, Falkowski1 PG (2017), Biological control of aragonite formation in stony

987   corals, Science 356, 933–938.

988   Wang J, Emile-Geay J, Guillot D, Smerdon JE, Rajaratnam B (2014), Evaluating climate field

989   reconstruction techniques using improved emulations of real-world conditions, Clim. Past, 10,

990   1–19.

991   Watanabe T, Gagan MK, Corrège T, Scott-Gagan H, Cowley J, Hantoro W (2003), Oxygen isotope

992   systematics in *Diploastrea heliopora*: New coral archive of tropical paleoclimate, Geochim.

993   Cosmochim. Acta, Vol. 67, No. 7, pp. 1349–1358.

994   Weber JN, Woodhead PMJ (1971), Diurnal variations in the isotopic composition of dissolved

995   inorganic carbon in seawater from coral reef environmens, Geochim. Cosmochim. Acta, 35,

996   891-902.

997   Weber JN, Woodhead PMJ (1972), Temperature dependence of Oxygen-18 concentration in reef coral

998   carbonates, J. Geophys. Res., *77,* 463-473.

999   Wei G, Deng W, Yu K, Li X, Sun W, Zhao J (2007), Sea surface temperature records in the northern

1000   South China Sea from mid-Holocene coral Sr/Ca ratios, Paleoceanography, 22, PA3206,

1001   doi:10.1029/2006PA001270.

1002   Worum FP, Carricart-Ganivat JP, Besnon L, Golicher D (2007), Simulation and observations of

1003   annual density banding in skeleton of *Montrastraea* (Cnidaria: Scleractinia) growing under

1004   thermal stress associated with ocean warming, Limn. Oceanogr., 52, 2317-2323.

1005   Wu HC, Linsley BK, Dassié EP, Schiraldi Jr. B, deMenocal BP (2013), Oceanographic variability in

1006   the South Pacific Convergence Zone region over the last 210 years from multi-site coral Sr/Ca

1007   records, Geochem. Geophys. Geosyst., 14, 1435–1453, doi:10.1029/2012GC004293.

1008   Zhang L, Chang P, Tippett MK (2009), Linking the Pacific Meridional Mode to ENSO: Utilization of

1009   a Noise Filter, J. Clim., 22, 905-921, DOI: 10.1175/2008JCLI2474.1.

39

1010   Zinke J, Rountrey A, Feng M, Xie SP, Dissard D, Rankenburg K, Lough JM, McCulloch MT (2014),

1011   Corals record long-term Leeuwin current variability including Ningaloo Niño/Niña since 1795,

1012   Nature Com., DOI: 10.1038/ncomms4607.

1013   Zhu X, Liu Z (2009), Tropical SST Response to Global Warming in the Twentieth Century, J. Cim.,

1014   22, 1305-1312, DOI: 10.1175/2008JCLI2164.1.

1015

1016

40

Table Captions

Table 1 – Groups of coral genera from WW72, identified as showing $\delta^{18}O$–temperature calibration constants linearly linked with correlation coefficient $R^2 \geq 0.99$ (Fig. 3). They have been first highlighted by calibrations forming bundle characterized by intersections defining $\delta^{18}O$ and temperature ranges (Fig. 1d).

Table 2 – Values of constant of $\delta^{18}O$–temperature calibrations from WW72, and from New Caledonia (Stephans et al., 2004), Clipperon (Linsley et al., 1999) and Indonesia (Maier et al., 2004).

41

1028 **Figure Captions**

1029

1030 **Figure 1** – Figures of the revisited Weber and Woodhead (1972) data series. **Fig. 1a** is the location of

1031 all the islands considered by the authors determining temperatures. **Fig. 1b** displays calibrations

1032 annual temperature–annual $\delta^{18}O$, plotted by considering annual temperature as the unknown

1033 parameters. **Fig. 1c** displays annual $\delta^{18}O$–annual temperature calibrations plotted with annual coral

1034 $\delta^{18}O$ as the unknown parameter, annual temperature being the robust parameter. **Fig. 1d** displays

1035 bundles of annual $\delta^{18}O$–annual temperature calibrations as we identify them from Fig. 1c, for the

1036 groups including *Porites* and *Acropora*. From Fig. 1d, it is possible to generate annual temperature

1037 and annual $\delta^{18}O$ ranges corresponding to the intersection of the calibrations. This feature is made

1038 possible by the homogenous light influence on calibrations.

1039

1040 **Figure 2** – Annual ($\delta^{18}O_{coral}$ - $\delta^{18}O_{seawater}$)-annual temperature calibrations. Weber and Woohead

1041 (1972) data series provided coral data. $\delta^{18}O_{seawater}$ are introduced in the annual $\delta^{18}O$-annual temperature

1042 calibrations according to Juillet-Leclerc and Schmidt (2001) method. Some genera are not present in

1043 all the sites, in turn at all temperatures and only corresponding $\delta^{18}O_{seawater}$ are introduced.

1044 *Acropora* $\delta^{18}O_{carbonate}$ - $\delta^{18}O_{Seawater}$ = –0.21 x SST (°C) + 1.26, R^2 = 0.87, n = 24, p<0.001

1045 *Porites* $\delta^{18}O_{carbonate}$ - $\delta^{18}O_{Seawater}$ = –0.20 x SST (°C) + 0.45, R^2 = 0.83, n = 22, p<0.001

1046 *Montipora* $\delta^{18}O_{carbonate}$ - $\delta^{18}O_{seawater}$ = –0.19 x SST (°C) + 0.64, R^2 = 0.64, n = 12, p<0.05

1047 *Platygira* $\delta^{18}O_{carbonate}$ - $\delta^{18}O_{seawater}$ = –0.19 x SST (°C) – 0.08, R^2 = 0.93, n = 11, p<0.001

1048 *Pavona* $\delta^{18}O_{carbonate}$ - $\delta^{18}O_{seawater}$ = –0.17 x SST (°C) – 0.47, R^2 = 0.87, n = 8, p<0.01

1049 Discrepancies between the different genera calibrations are related to microstructure distribution

1050 characterizing each morphology.

1051

1052 **Figure 3** – Linear relationship between (b) and (a), constants of the annual $\delta^{18}O$–annual temperature

1053 calibrations, $\delta^{18}O_{carbonate}$ = a x SST (°C) + b. Weber and Woohead (1972) data series provided coral

1054   data. **Fig. 3a** displays constants values from the 44 coral genera of Table 1. (a) is considered as the

1055   disequilibrium indicator compared to –0.19, the slope value derived from the theoretical $\delta^{18}O$–

1056   temperature relationship at equilibrium (Kim et al., 2007). The relationship b = –29.07 x a – 5.13, R^2 =

1057   0.95, n = 44, p<0.001 (the green line) takes into account all the data (dark green diamonds), whereas b

1058   = –27.94 x a – 4.84, R^2 = 0.90, n = 40, p<0.001 (the blue line) is assessed without the 4 extreme data

1059   (the remaining data are the blue crosses). On **Fig. 3b**, the dots are similar to the dots displayed on Fig.

1060   3a, however, color of the dots corresponds to the color of the calibration bundles of Fig. 1c.

1061   Group I   b = –24.43 x a – 4.18, R^2 = 0.99, n = 9, p<0.001 (the orange line)

1062   Group II   b = –26.63 x a – 4.91, R^2 = 0.99, n = 8, p<0.001 (the violin line)

1063   Group III   b = –25.85 x a – 4.10, R^2 = 0.99, n = 7, p<0.001 (the blue line)

1064   *Acropora* Group IV   b = –25.60 x a – 3.79, R^2 = 0.99, n = 10, p<0.001 (the green line)

1065   *Porites* Group V   b = –28.40 x a – 5.16, R^2 = 0.999, n = 9, p<0.001 (the brown line)

1066 $T_{intersection}$ and $\delta_{intersection}$ are only given for *Acropora* and *Porites* groups.

1067   Correlation coefficient of all the linear relationships are very high. All genera included in each group

1068   share identical microstructure distribution due to common feature of morphology.

1069

1070   **Figure 4** –Graphs derived from Stephans et al. (2004) data, available on NOAA (National Climatic

1071   Data Center site) (https://www.ncdc.noaa.gov/paleo/study/1877). On **Fig. 4a** are reported seasonal

1072   isotopic profiles from 1967 to 1993 period for 92PAC coral core (blue curve), 92PAD coral core (pink

1073   curve), 99PAA coral core (green curve) and 92PAA coral core (violin curve). All the cores have been

1074   harvested at Fort Amédée lighthouse proximity. Seasonal isotopic profiles are strongly impacted by

1075   seasonality with different light influence. **Fig. 4b** displays seasonal $\delta^{18}O$-seasonal temperature (GISS

1076   SST) calibrations for the coral cores studied.

1077   92PAC $\delta^{18}O_{carbonate}$ = – 0.17 x SST (°C) – 0.08, R^2 = 0.77, n = 296, p<0.001, blue curve

1078   99PAA $\delta^{18}O_{carbonate}$ = – 0.16 x SST (°C) – 0.39, R^2 = 0.67, n = 296, p<0.001, green curve

1079   92PAC $\delta^{18}O_{carbonate}$ = –0.15 x SST (°C) – 0.62, R^2 = 0.62, n = 296, p<0.001, violin curve

1080   92PAD $\delta^{18}O_{carbonate}$ = – 0.14 x SST (°C) – 1.09, R^2 = 0.59, n = 296, p<0.001, pink curve

1081   All (a) are higher than –0.19, the slope value derived from the theoretical $\delta^{18}O$–

1082   temperature relationship at equilibrium (Kim et al., 2007). These values indicate that fibers are the

1083   prevailing microstructures of the corals considered.

1084   **Fig. 4c** displays constant (a) and (b) relationship b = –32.6 x a – 5.6, R^2 = 0.98, n = 4, p<0.01.

1085

1086   **Figure 5** – Clipperton $\delta^{18}O$ data covering the period 1985–1994 (Linsley et al., 1999, 2000),

1087   available on https://www.ncdc.noaa.gov/paleo/study/1846. Three cores are considered 2B, 3C and 4B.

1088   **Fig. 5a** displays $\delta^{18}O$ profiles characterized by strong annual variability, 2B (orange curve), 3C (green

1089   curve), and 4B (blue curve). **Fig. 5b** shows the three core seasonal $\delta^{18}O$–monthly temperature

1090   calibrations.

1091   3C $\delta^{18}O_{carbonate}$ = –0.39 x SST (°C) + 5.26, trend graph derived from 3 temperatures, orange curve

1092   3C $\delta^{18}O_{carbonate}$ = –0.46 x SST (°C) + 7.4, trend graph derived from 3 temperatures, green curve

1093   4B $\delta^{18}O_{carbonate}$ = –0.53 x SST (°C) + 9.21, trend graph derived from 3 temperatures, blue curve

1094   The slope values (a) being lower than –0.19, the slope value derived from the theoretical $\delta^{18}O$–

1095   temperature relationship at equilibrium (Kim et al., 2007), correspond to coral colonies grown at high

1096   temperature showing great amount of COC compared to fiber amount.

1097   **Fig. 5c** displays constant (a) and (b) relationship b = –28.21 x a + 20.27, R^2 = 0.997, n = 3, p<0.01

1098

1099   **Figure 6** – 6 coral heads representing 3 *Porites* species (*Porites lutea*, *Porites murrayensis* and

1100   *Porites australiensis*), collected in Taka Bone Rate (Indonesia), have been sampled. Each species,

1101   composed by two coral heads, provides four sampling profiles covering 4 years. Each trajectory

1102   presents different light incidence. **Fig.6a** shows all the calibrations. Except one calibration of *Porites*

1103   *australiansis*, all the other calibrations exhibit intersection close to the temperature and $\delta^{18}O$ ranges

1104   defined for *Porites* group (Fig. 1d). All the calibrations constants are reported on **Fig. 6b**.

1105   The negative values (a), associated to high linear extension are characteristic features of coral skeleton

1106   grown at high temperature richer in COC than fibres. The correlation coefficient given for all *Porites*

1107   species is high: b = –28.34 x a – 5.59, R^2 = 0.999, n = 12, p<0.001

44

1108

1109 **Figure 7** – **Fig. 7a** displays *Porites* seasonal $\delta^{18}O$–monthly temperature calibrations of New

1110 Caledonia corals (Quinn and Sampson, 2002; Stephans et al., 2004), Clipperton corals (Linsey et al.,

1111 1999, 2000), Taka Bone Rate corals (Maier et al., 2004) and annual $\delta^{18}O$–annual temperature

1112 calibration derived from Weber and Woodhead (1972) data series. On **Fig. 7b** are plotted all the (a)

1113 and (b) values corresponding to the calibrations reported on Fig. 7a. The correlation coefficient given

1114 for all *Porites* species is high: b = –27.24 x a – 4.92, R^2 = 0.999, n = 30, p<0.001. All dots showing (a)

1115 > –0.19, the slope value derived from the theoretical $\delta^{18}O$–temperature relationship at equilibrium

1116 (Kim et al., 2007) correspond to New Caledonia coral cores developed at mitigated temperatures, with

1117 fibers in greater amounts compared to COC, all other ones showing (a) < –0.19 are associated to corals

1118 grown at high temperature, with reverse microstructures relative amounts.

1119

1120 **Figure 8** – Comparison of $\delta^{18}O$ measured on coral core collected at Moorea (French Polynesia)

1121 (Boiseau et al., 1998) and measured and estimated temperatures. On the left side **Fig. 8a**, between

1122 1980 and 1990, the seasonal measured data are compared to the instrumental seawater temperature

1123 (Boiseau et al., 1998). On the right side **Fig. 8b**, over the last century, the annual averaged measured

1124 data, originated from the same data series than seasonal data, are compared to the temperature

1125 estimated in the (1°, 1°) grid containing Moorea (Kaplan et al., 1998). The two curves are displayed to

1126 obtain the best matching. The isotopic scale of the two isotopic profiles is common to the two profiles,

1127 while the measured and the estimated temperature scales cover 7°C and 2°C respectively. There is a

1128 mismatch between the annual and monthly calibrations given on a unique isotopic scale, illustrating

1129 the non-linearity between the monthly and annual $\delta^{18}O$ profiles over the time.

1130

1131 **Figure 9** – Comparison of the monthly composite $\delta^{18}O$–monthly composite temperature calibration

1132 calculated over 1979 to 1989 (Fig. 9a) and the annual $\delta^{18}O$–annual temperature calibration calculated

1133 over 33 years (from 1989 to 1956) (Fig. 9b) (Boiseau et al., 1998). The averaged temperature

1134 calculated from the composite temperature is 25.88 °C whereas the averaged temperature from the last

45

1135   30 years is 26.7 °C. (a) of the monthly composite δ^{18}O–monthly composite temperature calibration

1136   shown on **Fig. 9a** is –0.15 similar with slope obtained from New Caledonia, however, the composite

1137   temperatures may not be really compared with the measurements. **Fig. 9b** displays the annual δ^{18}O–

1138   annual temperature calibration with the slope (a) slightly lower than –0.19 the slope value derived

1139   from the theoretical δ^{18}O–temperature relationship at equilibrium (Kim et al., 2007) in good

1140   agreement with the values reported on Fig. 7b.

1141

1142

Genus	Family	Suborder	Group	δ¹⁸O and temperature ranges SST °C	δ¹⁸O‰ vs VPDB	R=Specimen nb/Site nb	b	a
Platygyra	Faviidae	FA				8.23	2.24	-0.27
Leptoria	Faviidae	FA				3.36	2.37	-0.27
Goniopora	Poritidae	FU				6.46	0.99	-0.21
Goniastrea	Faviidae	FA	I	24.42	-4.18	7.00	1.72	-0.24
Echinophyllia	Faviidae	FA				2.14	2.29	-0.26
Oxypora	Pectiniidae	FA				1.80	1.32	-0.22
Astreopora	Fungiidae	A				4.67	0.72	-0.20
Favites	Faviidae	FA				6.55	1.67	-0.24
Plesiastrea	Faviidae	FA				6.00	1.82	-0.24
Coeloseris	Agariciidae	FU				4.80	-0.48	-0.17
Caulastrea	Faviidae	FA				3.00	2.96	-0.30
Acrhelia	Faviidae	FA				2.50	0.44	-0.20
Oulophyllia	Faviidae	FA	II	26.63	-4.91	2.50	-1.68	-0.12
Lobophyllia	Mussidae	FA				7.07	0.92	-0.22
Symphyllia	Mussidae	FA				3.75	1.09	-0.22
Favia	Faviidae	FA				6.56	1.53	-0.24
Acanthastrea	Mussidae	FA				2.30	2.72	-0.28
Pavona	Agariciidae	FU				7.94	2.18	-0.25
Alveopora	Poritidae	FU				3.40	1.44	-0.21
Diploastrea	Faviidae	FA				2.17	2.11	-0.24
Cyphastrea	Faviidae	FA	III	25.85	-4.10	3.81	1.08	-0.20
Fungia	Fungiidae	FU				13.62	2.74	-0.26
Polyphyllia	Fungiidae	FU				2.57	1.24	-0.21
Leptastrea	Fungiidae	FU				5.21	2.01	-0.23
Pliesioseris	Thamnastreiidae	A				3.40	2.08	-0.23
Psammocora	Thamnastreiidae	A				5.87	2.03	-0.23
Parahalomitra	Fungiidae	FU				2.56	3.99	-0.31
Coscinarea	Siderastreiidae	FU				3.43	2.85	-0.26
Herpolitha	Fungiidae	FU				2.22	5.39	-0.36
Seriatopora	Pocilloporidae	A	IV	25.6	-3.79	4.44	3.11	-0.27
Stephanaria	Thamnastreiidae	A				1.89	4.10	-0.31
Turbinaria	Dendrophyllidae	D				6.43	4.01	-0.30
Montipora	Acroporidae	A				11.70	3.76	-0.29
Acropora	Acroporidae	A				30.93	3.43	-0.28
Stylophora	Pocilloporidae	A				6.80	2.02	-0.22
Euphyllia	Caryophylliidae	C				5.11	0.60	-0.20
Merulina	Merulinidae	FA				3.75	0.68	-0.21
Pectinea	Pectiniidae	FA				2.80	-0.58	-0.16
Galaxea	Oculinidae	FA				5.07	1.98	-0.25
Hydnophora	Faviidae	FA	V	28.4	-5.16	3.89	2.87	-0.28
Echinopora	Faviidae	FA				5.27	2.93	-0.28
Porites	Poritidae	FU				16.19	3.39	-0.30
Pocillopora	Acroporidae	A				9.33	2.37	-0.26
Mycedium	Pectiniidae	FA				2.00	3.87	-0.32

1143
1144
1145 **Table 1** – Groups of coral genera from WW72, identified as showing δ¹⁸O–temperature calibration

1146 constants linearly linked with correlation coefficient $R^2 \geq 0.99$ (Fig. 3). They have been first

1147 highlighted by calibrations forming bundle characterized by intersections defining δ¹⁸O and

1148 temperature ranges (Fig. 1d).

1149

47

1150
1151

	$\delta^{18}O = a*SST + b$	
	a	b
	-0.20	0.60
	-0.21	0.68
	-0.16	-0.58
	-0.25	1.98
from WW72	-0.28	2.87
	-0.28	2.93
	-0.30	3.39
	-0.26	2.37
	-0.32	3.87
	-0.17	-0.08
from Stephans et al., 2004	-0.16	-0.39
	-0.15	-0.62
	-0.14	-1.09
	-0.46	7.4
from Linsley et al., 1999	-0.53	9.21
	-0.39	5.26
	-0.78	16.29
	-0.80	17.06
	-0.56	10.29
	-0.61	11.86
	-0.59	11.17
from Maier et al., 2004	-0.47	7.76
	-0.47	7.58
	-0.43	6.83
	-0.51	8.91
	-0.38	5.10
	-0.93	20.92
	-0.43	6.35

1152
1153
1154
1155
1156 **Table 2** – Values of constant of $\delta^{18}O$–temperature calibrations from WW72, and from New

1157 Caledonia (Stephans et al., 2004), Clipperon (Linsley et al., 1999) and Indonesia (Maier et al., 2004).

1158

48

1159
1160
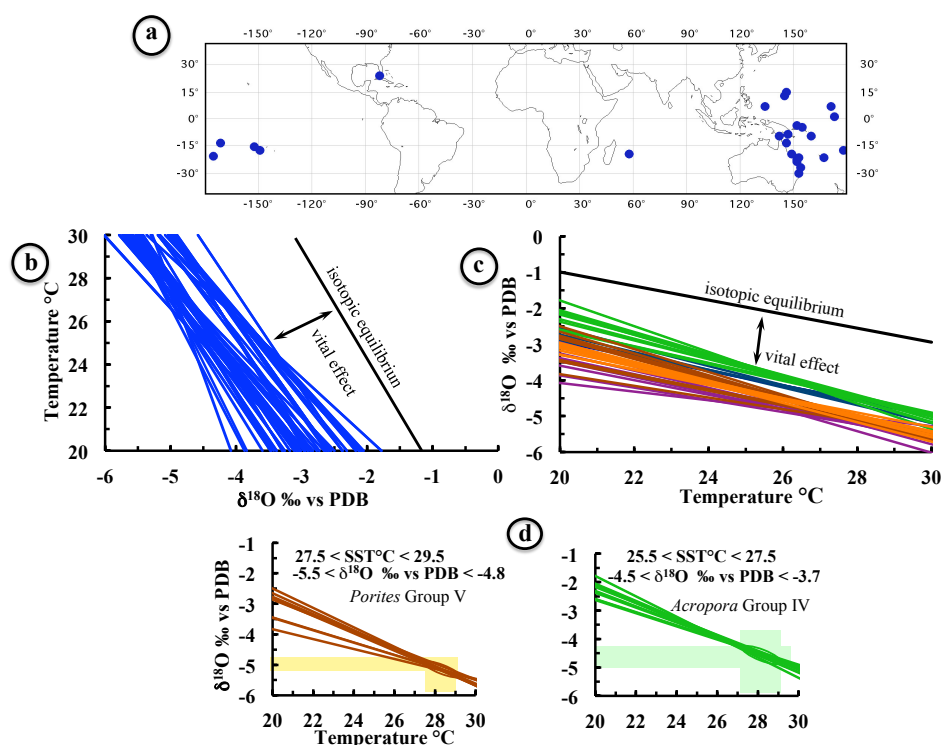
1161
1162
1163   **Figure 1** – Figures of the revisited Weber and Woodhead (1972) data series. **Fig. 1a** is the location of

1164   all the islands considered by the authors determining temperatures. **Fig. 1b** displays calibrations

1165   annual temperature–annual $\delta^{18}O$, plotted by considering annual temperature as the unknown

1166   parameters. **Fig. 1c** displays annual $\delta^{18}O$-annual temperature calibrations plotted with annual coral

1167 $\delta^{18}O$ as the unknown parameter, annual temperature being the robust parameter. **Fig. 1d** displays

1168   bundles of annual $\delta^{18}O$-annual temperature calibrations as we identify them from Fig. 1c, for the

1169   groups including *Porites* and *Acropora*. From Fig. 1d, it is possible to generate annual temperature

1170   and annual $\delta^{18}O$ ranges corresponding to the intersection of the calibrations. This feature is made

1171   possible by the homogenous light influence on calibrations.

1172

49

1173
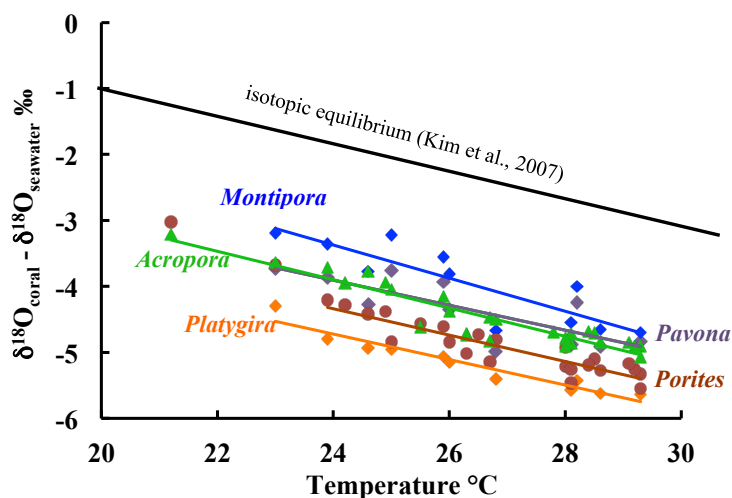
1174
1175
1176 **Figure 2** – Annual ($\delta^{18}O_{coral} - \delta^{18}O_{seawater}$)-annual temperature calibrations. Weber and Woohead

1177 (1972) data series provided coral data. $\delta^{18}O_{seawater}$ are introduced in the annual $\delta^{18}O$-annual temperature

1178 calibrations according to Juillet-Leclerc and Schmidt (2001) method. Some genera are not present in

1179 all the sites, in turn at all temperatures and only corresponding $\delta^{18}O_{seawater}$ are introduced.

1180 *Acropora* $\delta^{18}O_{carbonate} - \delta^{18}O_{seawater} = -0.21 \times SST\ (°C) + 1.26$, $R^2 = 0.87$, $n = 24$, $p<0.001$

1181 *Porites* $\delta^{18}O_{carbonate} - \delta^{18}O_{seawater} = -0.20 \times SST\ (°C) + 0.45$, $R^2 = 0.83$, $n = 22$, $p<0.001$

1182 *Montipora* $\delta^{18}O_{carbonate} - \delta^{18}O_{seawater} = -0.19 \times SST\ (°C) + 0.64$, $R^2 = 0.64$, $n = 12$, $p<0.05$

1183 *Platygira* $\delta^{18}O_{carbonate} - \delta^{18}O_{seawater} = -0.19 \times SST\ (°C) - 0.08$, $R^2 = 0.93$, $n = 11$, $p<0.001$

1184 *Pavona* $\delta^{18}O_{carbonate} - \delta^{18}O_{seawater} = -0.17 \times SST\ (°C) - 0.47$, $R^2 = 0.87$, $n = 8$, $p<0.01$

1185 Discrepancies between the different genera calibrations are related to microstructure distribution

1186 characterizing each morphology.

1187

1188
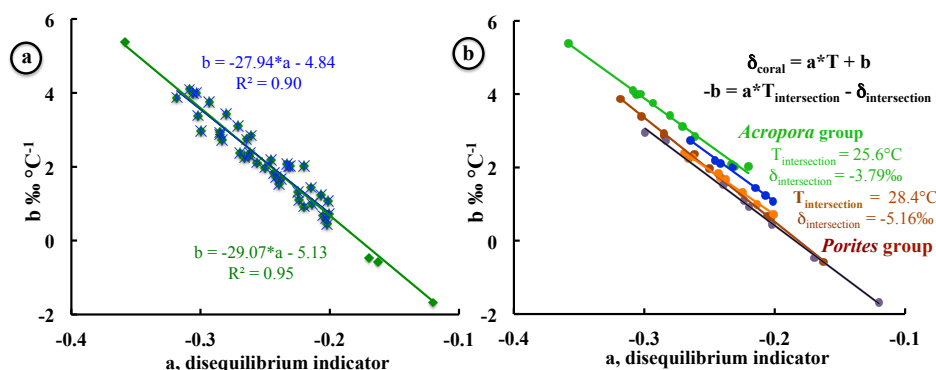
1189
1190
1191   **Figure 3** – Linear relationship between (b) and (a), constants of the annual δ^{18}O-annual temperature

1192   calibrations, $\delta^{18}O_{carbonate}$ = a x SST (°C) + b. Weber and Woohead (1972) data series provided coral

1193   data. **Fig. 3a** displays constants values from the 44 coral genera of Table 1. (a) is considered as the

1194   disequilibrium indicator compared to –0.19, the slope value derived from the theoretical δ^{18}O-

1195   temperature relationship at equilibrium (Kim et al., 2007). The relationship b = –29.07 x a – 5.13, R^2 =

1196   0.95, n = 44, p<0.001 (the green line) takes into account all the data (dark green diamonds), whereas b

1197   = –27.94 x a – 4.84, R^2 = 0.90, n = 40, p<0.001 (the blue line) is assessed without the 4 extreme data

1198   (the remaining data are the blue crosses). On **Fig. 3b**, the dots are similar to the dots displayed on Fig.

1199   3a, however, color of the dots corresponds to the color of the calibration bundles of Fig. 1c.

1200   Group I   b = –24.43 x a – 4.18, R^2 = 0.99, n = 9, p<0.001 (the orange line)

1201   Group II   b = –26.63 x a – 4.91, R^2 = 0.99, n = 8, p<0.001 (the violin line)

1202   Group III   b = –25.85 x a – 4.10, R^2 = 0.99, n = 7, p<0.001 (the blue line)

1203   *Acropora* Group IV   b = –25.60 x a – 3.79, R^2 = 0.99, n = 10, p<0.001 (the green line)

1204   *Porites* Group V   b = –28.40 x a – 5.16, R^2 = 0.999, n = 9, p<0.001 (the brown line)

1205 $T_{intersection}$ and $\delta_{intersection}$ are only given for *Acropora* and *Porites* groups.
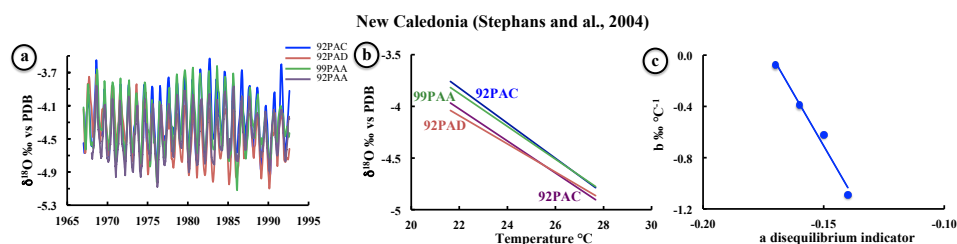
1206   Correlation coefficient of all the linear relationships are very high. All genera included in each group

1207   share identical microstructure distribution due to common feature of morphology.

1208

51

Figure 4 –Graphs derived from Stephans et al. (2004) data, available on NOAA (National Climatic

Data Center site) (https://www.ncdc.noaa.gov/paleo/study/1877). On **Fig. 4a** are reported seasonal

isotopic profiles from 1967 to 1993 time period for 92PAC coral core (blue curve), 92PAD coral core

(pink curve), 99PAA coral core (green curve) and 92PAA coral core (violin curve). All the cores have

been harvested at Fort Amédée lighthouse proximity. Seasonal isotopic profiles are strongly impacted

by seasonality with different light influence. **Fig. 4b** displays seasonal δ^{18}O–seasonal temperature

(GISS SST) calibrations for the coral cores studied.

92PAC $\delta^{18}O_{carbonate} = -0.17$ x SST (°C) $- 0.08$, $R^2 = 0.77$, n = 296, p<0.001, blue curve

99PAA $\delta^{18}O_{carbonate} = -0.16$ x SST (°C) $- 0.39$, $R^2 = 0.67$, n = 296, p<0.001, green curve

92PAC $\delta^{18}O_{carbonate} = -0.15$ x SST (°C) $- 0.62$, $R^2 = 0.62$, n = 296, p<0.001, violin curve

92PAD $\delta^{18}O_{carbonate} = -0.14$ x SST (°C) $- 1.09$, $R^2 = 0.59$, n = 296, p<0.001, pink curve

All (a) are higher than -0.19, the slope value derived from the theoretical δ^{18}O-

temperature relationship at equilibrium (Kim et al., 2007). These values indicate that fibers are the

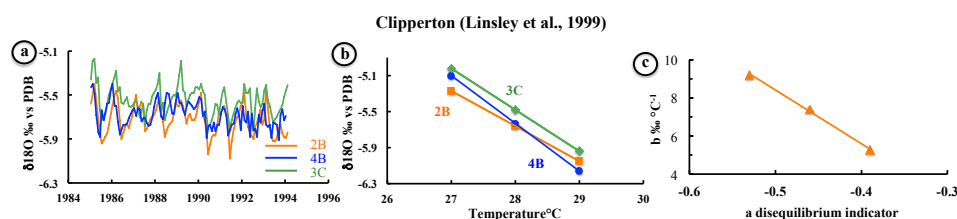prevailing microstructures of the corals considered.

Fig. 4c displays constant (a) and (b) relationship b = -32.6 x a $- 5.6$, $R^2 = 0.98$, n = 4, p<0.01.

52

1227
1228
1229 **Figure 5** – Clipperton $\delta^{18}O$ data covering 1985-1994 period (Linsley et al., 1999, 2000), available on

1230 https://www.ncdc.noaa.gov/paleo/study/1846. Three cores are considered 2B, 3C and 4B. **Fig. 5a**

1231 displays $\delta^{18}O$ profiles characterized by strong annual variability, 2B (orange curve), 3C (green curve),

1232 and 4B (blue curve). **Fig. 5b** shows the three core seasonal $\delta^{18}O$–monthly temperature calibrations.

1233 3C $\delta^{18}O_{carbonate} = -0.39$ x SST (°C) + 5.26, trend graph derived from 3 temperatures, orange curve

1234 3C $\delta^{18}O_{carbonate} = -0.46$ x SST (°C) + 7.4, trend graph derived from 3 temperatures, green curve

1235 4B $\delta^{18}O_{carbonate} = -0.53$ x SST (°C) + 9.21, trend graph derived from 3 temperatures, blue curve

1236 The slope values (a) being lower than –0.19, the slope value derived from the theoretical $\delta^{18}O$-

1237 temperature relationship at equilibrium (Kim et al., 2007), correspond to coral colonies grown at high

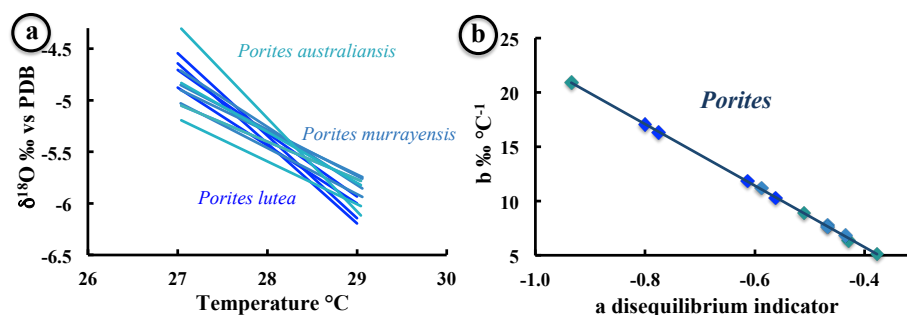1238 temperature showing great amount of COC compared to fibre amount.

1239 **Fig. 5c** displays constant (a) and (b) relationship b = –28.21 x a + 20.27, R^2 = 0.997, n = 3, p<0.01

1240
1241

53

1242

Taka Bone Rate (Indonesia) (Maier et al., 2004)


1243
1244
1245 **Figure 6** – 6 coral heads representing 3 *Porites* species (*Porites lutea*, *Porites murrayensis* and

1246 *Porites australiensis*), collected in Taka Bone Rate (Indonesia), have been sampled. Each species,

1247 composed by two coral heads, provides four sampling profiles covering 4 years. Each trajectory

1248 presents different light incidence. **Fig.6a** shows all the calibrations. Except one calibration of *Porites*

1249 *australiansis*, all the other calibrations exhibit intersection close to the temperature and δ^{18}O ranges

1250 defined for *Porites* group (Fig. 1d). All the calibrations constants are reported on **Fig. 6b**.

1251 The negative values (a), associated to high linear extension are characteristic features of coral skeleton

1252 grown at high temperature richer in COC than fibres. The correlation coefficient given for all *Porites*

1253 species is high: b = –28.34 x a – 5.59, R^2 = 0.999, n = 12, p<0.001

1254

54

1255
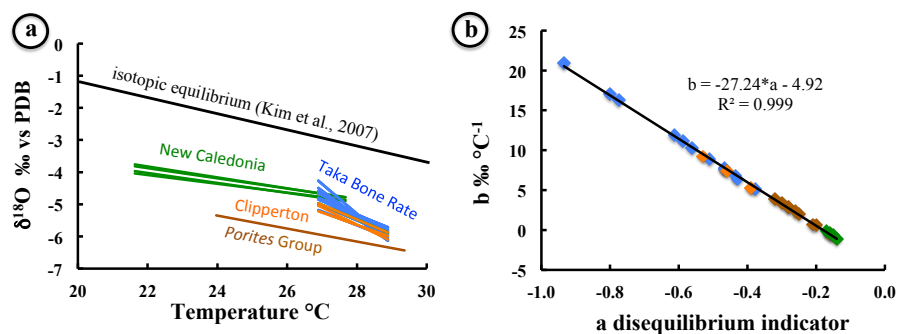
1256
1257
1258 **Figure 7** – **Fig. 7a** displays *Porites* seasonal δ^{18}O-monthly temperature calibrations of New

1259 Caledonia corals (Quinn and Sampson, 2002; Stephans et al., 2004), Clipperton corals (Linsey et al.,

1260 1999, 2000), Taka Bone Rate corals (Maier et al., 2004) and annual δ^{18}O-annual temperature

1261 calibration derived from Weber and Woodhead (1972) data series. On **Fig. 7b** are plotted all the (a)

1262 and (b) values corresponding to the calibrations reported on Fig. 7a. The correlation coefficient given

1263 for all *Porites* species is high: b = –27.24 x a – 4.92, R^2 = 0.999, n = 30, p<0.001. All dots showing (a)

1264 > –0.19, the slope value derived from the theoretical δ^{18}O-temperature relationship at equilibrium

1265 (Kim et al., 2007) correspond to New Caledonia coral cores developed at mitigated temperatures, with

1266 fibers in greater amounts compared to COC, all other ones showing (a) < –0.19 are associated to corals

1267 grown at high temperature, with reverse microstructures relative amounts.

1268

55

1269
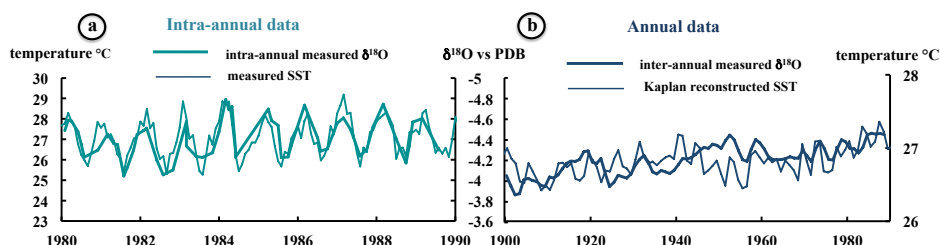
1270
1271
1272 **Figure 8** – Comparison of δ¹⁸O measured on coral core collected at Moorea (French Polynesia)

1273 (Boiseau et al., 1998) and measured and estimated temperatures. On left hand **Fig. 8a**, between 1980

1274 and 1990, seasonal measured data are compared to instrumental seawater temperature (Boiseau et al.,

1275 1998). On right hand **Fig. 8b**, over the last century, annual averaged measured data, originated from

1276 the same data series than seasonal data, are compared to estimated temperature in the (1°, 1°) grid

1277 containing Moorea (Kaplan et al., 1998). The two curves are displayed to obtain the best matching.

1278 Isotopic scale of the two isotopic profiles is common to the two profiles, while measured and

1279 estimated temperature scales cover 7°C and 2°C respectively. There is a mismatch between annual and
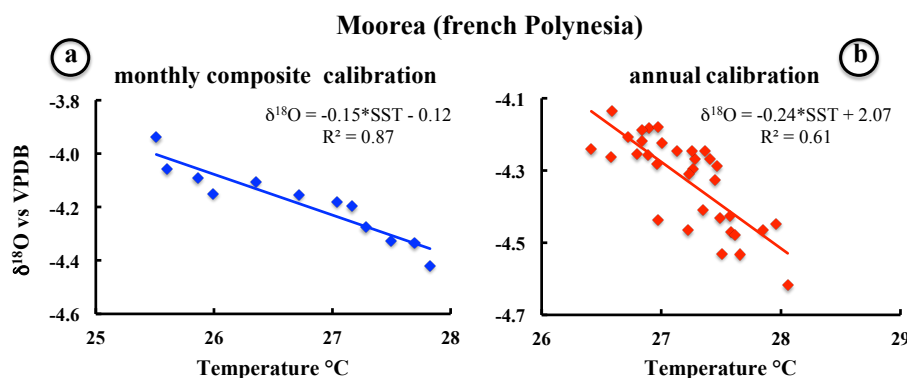
1280 monthly calibrations given on a unique isotopic scale, illustrating the non-linearity between monthly

1281 and annual δ¹⁸O profiles over the time.

1282

56

1283

1284
1285
1286   **Figure 9** – Comparison of monthly composite δ^{18}O-monthly composite temperature calibration

1287   calculated over 1979 to 1989 (Fig. 9a) and annual δ^{18}O-annual temperature calibration calculated over

1288   33 years (from 1989 to 1956) (Fig. 9b) (Boiseau et al., 1998). Averaged temperature calculated from

1289   composite temperature is 25.88 °C whereas averaged temperature from the last 30 years is 26.7 °C. (a)

1290   of the monthly composite δ^{18}O-monthly composite temperature calibration shown on **Fig. 9a** is –0.15

1291   similar with slope obtained from New Caledonia, however, composite temperatures may not be really

1292   compared with measurements. **Fig. 9b** displays annual δ^{18}O-annual temperature calibration with slope

1293   (a) slightly lower than –0.19 the slope value derived from the theoretical δ^{18}O-temperature relationship

1294   at equilibrium (Kim et al., 2007) in good agreement with values reported on Fig. 7b.

1295